Spin wave modes of multilayered ferromagnetic films

I. A. Armijo and R. E. Arias
Departamento de Física, CEDENNA, Facultad de Ciencias Físicas y Matemáticas, Universidad de Chile, Santiago, Chile

(Received 14 September 2018; revised manuscript received 31 December 2018; published 25 January 2019)

A study of ferromagnetic spin wave modes in multilayered films under general conditions is presented within a micromagnetic approximation. These modes, either in the magnetostatic or dipole-exchange approximation, have been studied in the past theoretically and experimentally by several authors. The novelty of the present study is that using a method based on the extinction-Green theorems it is possible to determine these modes with ease, under an arbitrary direction of an applied dc magnetic field, and for boundary conditions of diverse nature. The ferromagnetic films are coupled through dipolar interactions and eventually through exchange interactions. Due to an assumed in-plane translation invariance of the multilayers, the method allows us to determine the eigenfrequencies at a given in-plane wave vector as an algebraic eigenvalue problem of reasonable size: it is a $6N \times 6N$ system of homogeneous equations if there are N distinct films in the structure. Examples of modes in different multilayers are presented. If the stack of films is symmetric with respect to a central plane, it is shown that there are modes reciprocal in frequency but nonreciprocal in shape with respect to a change of sign of the wave vector. The latter is a generalization of the well-known shape nonreciprocity of Damon-Eshbach surface modes moving in opposite directions, and is valid for all dipole-exchange modes and inclined applied magnetic fields. The possibility of obtaining dispersion relations for obliquely applied magnetic fields should be of interest in order to test experimentally boundary conditions that model physical mechanisms operating at the different surfaces and interfaces of the films.

DOI: 10.1103/PhysRevB.99.014432

I. INTRODUCTION

The geometry of extended thin films has been very important in ferromagnetism. One could say that it was the first geometry to be extensively studied experimentally, and presently it continues to play a major role since it is quite ubiquitous in several structures and devices of interest. The following natural extension of a single film was multilayers of films of different characteristics and materials. These stacks of films allowed us to engineer metamaterials with properties that may be tuned to some extent to the interest of the designer. In particular, modern growth techniques of materials started with multilayered stacks of films, and then proceeded to nanowires and nanoparticles that are presently under close investigation. In the area of multilayers of films, a particular interest has been to determine the type and extent of coupling between different films: in general there are dipolar interactions, but depending on the separation between the ferromagnetic films and the intervening material, there may be an exchange coupling between layers that may be of ferromagnetic or antiferromagnetic character.

The study of spin wave modes in ferromagnetic multilayered films has been an area of active research interest for several decades now, both due to its own merit and also as a practical means to determine the underlying physical properties of the films involved and of their interactions. Thus, critical parameters of the models of magnetization dynamics of multilayers of ferromagnetic films may be determined through their imprint on the behavior of the spin wave modes of the multilayers. For example, surface anisotropies or interfacial exchange coupling constants may be determined through examination of spin wave modes characteristics.

By now there is a substantial body of work on the subject of spin wave modes in multilayers of ferromagnetic films. In the following we mention a few representative works on the subject, it is not an exhaustive list. To start, a very important background on this subject are studies of spin wave modes in single ferromagnetic films: we mention early works on magnetostatic modes [1,2] and dipole-exchange modes [3,4], and newer studies using a microscopic Heisenberg model [5] and a new long wavelengths model [6], with an interest in Bose-Einstein condensation and superfluidity of magnons [7]. Now the first studies in ferromagnetic multilayers were on magnetostatic modes, with long wavelengths on the order of micrometers: Ref. [8] is a theoretical-experimental work on N magnetized in-plane films with magnetostatic mode propagation perpendicular to the magnetization, Ref. [9] is a theoretical work on coupled magnetostatic modes in multilayers magnetized in-plane that also determines light scattering response, and Ref. [10] discusses detection of magnetostatic modes in bilayers via Brillouin light scattering. At the end of the 1980s and beginning of the 1990s there were several studies [11–18] on spin wave modes and their excitation in multilayers that also included the exchange interaction, i.e., dipole-exchange modes, and that considered surface and/or interfacial anisotropies, and an exchange interaction between layers. Most of the previous works used the so called partial waves approach to describe the magnetization dynamics inside the films, which goes back to the work of DeWames and Wolfram on a single film [3] (we comment on this method in Appendix A 1). At this point we mention that there are

some early works that developed a theory of the appropriate boundary conditions for the continuum micromagnetic theory approach to the magnetization dynamics in these multilayered films: they dealt with surface anisotropies [19,20] and with interlayer exchange coupling [21,22]. Later, at the beginning of the 1990s, some works [23–26] were published that discussed inconsistencies of the Hoffmann interlayer exchange coupling boundary conditions: this lead to the so called Barnas-Mills boundary conditions [25,26]. One could say that the core of the continuum micromagnetic theory of dipole-exchange spin wave modes in multilayered films had been established by then. In the following years the theory was extended in several directions like Brillouin light scattering studies in multilayers [27–29], layers with antiferromagnetic coupling and noncollinear magnetizations [30–32], magnonic crystals [33], etc. Also, we mention that some review papers have been published on the subject [34–36].

The present work shows quite general results on spin wave modes in multilayers of ferromagnetic films, within a continuum micromagnetic model for the magnetization dynamics, in the magnetostatic and dipole-exchange regimes. It corresponds to a generalization of similar results that were presented for a single film [37] to the case of multilayers of films. An advantage of the method used is that it allows us without much practical difficulty to calculate the details of the spin wave modes under general conditions, with a magnetic field applied at an arbitrary orientation with respect to the films, and different boundary conditions at the surfaces of the films. An assumption is that the equilibrium magnetization is uniform (effectively we assume weak effective fields with origin at the surfaces/interfaces). The method is based on an application of extinction-Green theorems [38–40] that allows us to write convolution integral equations for the modes, but that in the case of these multilayered films become local algebraic equations in wave-vector space due to translation invariance in the in-plane direction. The determination of the spin wave mode frequencies at a given wave vector requires solving an homogeneous eigenvalue problem that involves a $6N \times 6N$ matrix, where N is the number of films that form the multilayer structure (it can also be solved for a periodic structure, in which case the size of the system is associated with the number of films that form the basic repeated structure). The explicit general form of these equations is presented: it is simple to solve them in a particular case of interest due to the reasonable size of the system of equations and to the wide availability of numerical-graphical methods for solving it. Furthermore, the shapes of the collective modes at any location follow by a similar calculation. In particular, for stacks of films that are symmetric with respect to a central plane, we show by symmetry considerations that modes with a different sign of wave vector have the same frequencies, i.e., reciprocal in this sense, but their shapes are nonreciprocal: indeed the magnetostatic potential and magnetization components of these modes are, respectively, specular reflections and antireflections of each other with respect to the central plane. This is a generalization of the well-known shape nonreciprocity [41] of Damon-Eshbach surface modes [1] in a single ferromagnetic film, modes that move in opposite directions with the same frequencies but "attached" to the opposite surfaces.

In Sec. II we discuss the theory, i.e., the equations to be solved in order to determine the spin wave normal modes of the multilayered structures, and we introduce the method that uses the Green-extinction theorems to solve for these modes. In Sec. III we discuss exact relations between modes with opposite signs of their wave vectors in stacks of films that are symmetric with respect to a central plane, these results follow from symmetry considerations. In Sec. IV we discuss the boundary conditions that have been proposed in the literature in order to solve for the spin wave modes within the continuum micromagnetic approximation. In Sec. V we present numerical results on magnetostatic and dipole-exchange spin wave modes for selected cases. In Sec. VI we present some conclusions and final considerations. Finally, we have Appendix with details on some sections.

II. DIPOLE-EXCHANGE MODES OF FERROMAGNETIC MULTILAYERED FILMS

In the following we outline the theory used to determine the spin wave modes of multilayered films, within a continuous micromagnetic model. The dynamic equations that need to be solved correspond to the Landau-Lifshitz equations for the magnetization dynamics in each ferromagnetic film, combined with the magnetostatic equations needed to determine the magnetic field or magnetostatic potential everywhere. Thus, the determination of the spin wave modes in this geometry requires solving several coupled differential equations in different regions that are connected through appropriate boundary conditions.

We present a method that applied to this multilayered geometry allows us to calculate the spin wave modes with ease. It corresponds to an application of the Green-extinction theorems that allows us to formulate the eigenvalue problem in terms of integral equations written on the edges of the samples. In particular, it is assumed that these multilayered films are infinite in the in-plane directions, i.e., there is translation invariance in these directions. This means that due to the convolution theorem the latter integral equations become local algebraic equations in the in-plane wave vector space. This means, for example, that in the case of two coupled ferromagnetic films, the determination of the spin wave mode frequencies, at a given in-plane wave vector, involves solving an algebraic eigenvalue problem associated with a 12×12 matrix, something that is numerically simple.

The mentioned method was introduced in Ref. [37] for the case of a single ferromagnetic film. In that case the method was used with reference to Green's functions. Following the experience gained in that work, in the present case we do not make reference to Green's functions explicitly, since from a practical point of view what was used there were the in-plane Fourier transforms of those Green's functions that indeed are exponential type solutions to the equations of motion in the different regions, at a given in-plane wave vector. Indeed, for writing integral equations at the edges of the samples with this method, one basically needs to do a convolution between the modes that one is seeking with any other complete set of solutions of the equations of motions in the particular subregion in question (for these multilayered films that are "infinite" in-plane these spatial convolutions become local

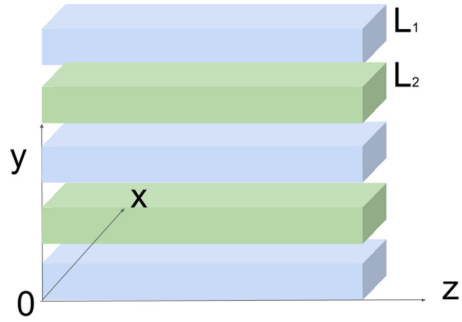

FIG. 1. A possible geometry: A stack of five ferromagnetic films separated by nonmagnetic spacers, two films are different from the rest.

equations in wave vector space). As a matter of convenience, in the following we will name these exponential solutions to the equations of motion as "auxiliary solutions."

In the following we describe the equations that need to be solved and the method we use in order to determine the spin wave modes of multilayered structures.

A. Spin wave modes

1. Equilibrium magnetization configuration and linear dynamic deviations

In the following we describe the geometry, the equilibrium magnetization configuration, and linear dynamic deviations from it.

With respect to the geometry, we consider ferromagnetic multilayered films, under several arrangements: it could be a pair of films or several films separated by nonmagnetic media; several films in contact; or a periodic concatenation of several films separated by nonmagnetic media or not. For example, Fig. 1 represents a stack of five films, separated by nonmagnetic media, with two of them of different characteristics.

We consider that there is a dc magnetic field applied to the stack of films, in a direction that in general is inclined with respect to the in-plane direction. We are assuming that the direction of the equilibrium magnetization is unaffected by surface torques that may arise (in principle, the equilibrium magnetization should curve a bit when approaching the surfaces of films when there is a magnetic field applied to the structure in an oblique direction), i.e., effectively we are assuming that those surface torques are weak. For example, in the case of existence of a surface anisotropy, the length A/K_s should be much longer than the thickness of the film (A and K_s are the exchange and surface anisotropy constants, proportional to the strength of the exchange and surface anisotropy energies, respectively). Under this approximation, the equilibrium magnetization configuration in each film is independent of the rest of the films, thus we present the angles of the applied magnetic film and the equilibrium magnetization for a single film of the structure in Fig. 2.

The applied magnetic field of magnitude H_0 makes an angle θ_H with respect to the $\hat{z}$ direction, which is parallel to the plane of the film. Thus, the equilibrium magnetization in layer (j) will be inclined at an angle θ_M^j with respect to the plane ($\theta_M^j < \theta_H$), defining the $\hat{\vec{z}}^j$ direction, i.e., $\vec{M}_{\rm eq} = M_s^j \hat{\vec{z}}^j$.

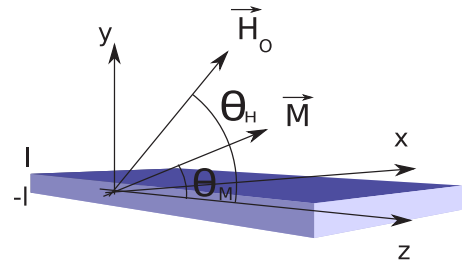

FIG. 2. Schematics of the equilibrium magnetization and applied magnetic field in a given film of the structure.

This inclined magnetization at layer (j) has an associated uniform internal magnetic field $\vec{H}_{\rm int}^j = H_0 \cos\theta_H \hat{z} + (H_0 \sin\theta_H - 4\pi M_s^j \sin\theta_M^j)\hat{y} = H_{int}^j \hat{\vec{z}}^j$, i.e., along the $\hat{\vec{z}}^j$ direction, since in equilibrium the magnetization at each film is parallel to the local internal magnetic field. These angles θ_M^j, θ_H are related through

$$\tan\theta_M^j = \frac{H_0 \sin\theta_H - 4\pi M_s^j \sin\theta_M^j}{H_0 \cos\theta_H}. \tag{1}$$

Furthermore, the linear dipole-exchange normal modes are eigensolutions of the Landau-Lifshitz equations for the linear magnetization dynamics coupled with the magnetostatic equations that determine the associated dipolar fields (when one includes the exchange interaction the magnetization satisfies appropriate boundary conditions on all the film surfaces). To linear approximation the magnetization in each film is expanded as

$$\begin{aligned}\vec{M}^j(\vec{x},t) &\simeq M_s^j \hat{\vec{z}}^j + \vec{m}^j(\vec{x},t) \\ &= M_s^j \hat{\vec{z}}^j + m_x^j(\vec{x},t)\hat{x} + m_{\hat{y}^j}^j(\vec{x},t)\hat{\vec{y}}^j,\end{aligned} \tag{2}$$

with $\hat{\vec{y}}^j$ and $\hat{x}$ directions perpendicular to the equilibrium magnetization direction $\hat{\vec{z}}^j$ in film (j). We will look for linear eigenmodes of frequency ω, i.e., $\vec{m}^j(\vec{x},t) = {\rm Re}[\vec{m}_\omega^j(\vec{x})\exp(-i\omega t)]$. We also introduce in-plane wave vectors $\vec{Q}$, so that $\vec{m}_j^\omega(\vec{x}) = \sum_{\vec{Q}} \vec{m}_j^{(\omega\vec{Q})} \exp(i\vec{Q}\cdot\vec{x})$, with $\vec{Q} = q\hat{x} + k\hat{z}$.

2. Magnetostatic equations

The spin wave normal modes have associated dynamic demagnetizing fields that satisfy the following magnetostatic equations everywhere:

$$\nabla\cdot\vec{b}^\omega = 0, \quad \nabla\times\vec{h}_D^\omega = 0, \tag{3}$$

with $\vec{b}^\omega$ and $\vec{h}_D^\omega$ the magnetic induction and demagnetizing fields, respectively, $\vec{b}_j^\omega = \vec{h}_j^\omega + 4\pi\vec{m}_j^\omega$ in the ferromagnetic material (j), and $\vec{b}^\omega = \vec{h}_D^\omega$ outside the films. The second equation $\nabla\times\vec{h}_D^\omega = 0$ is solved through the introduction of a magnetostatic potential, i.e., $\vec{h}_D^\omega = -\nabla\phi^\omega$, which is valid everywhere. The first equation $\nabla\cdot\vec{b}^\omega = 0$ implies that outside the films:

$$0 = \nabla^2\phi_\omega, \tag{4}$$

and inside film (j):

$$0 = -\nabla^2\phi_j^\omega + \frac{1}{2}\left[\left(\frac{\partial}{\partial x} - i\frac{\partial}{\partial \tilde{y}}\right)M_+^{\omega j} + \left(\frac{\partial}{\partial x} + i\frac{\partial}{\partial \tilde{y}}\right)M_-^{\omega j}\right]. \tag{5}$$

The following definitions were introduced: $m_\pm^j \equiv m_x^j \pm im_{\tilde{y}^j}^j \equiv M_\pm^j/4\pi$. The magnetostatic equations are to be solved with their associated boundary conditions at every interface, which are continuity of the normal component of $\vec{b}^\omega$ and the tangential component of $\vec{h}^\omega$ or equivalent continuity of the magnetostatic potential ϕ^ω.

3. Magnetization dynamics, Landau-Lifshitz equation

In our micromagnetic model the energy of the system is the sum of the energies of each film (j) given by

$$E_j = \int_{V_j} dV \left\{ \frac{A_j}{\left(M_s^j\right)^2}(\nabla\vec{M})^2 - \frac{1}{2}\vec{H}_D(\vec{M})\cdot\vec{M} - \vec{H}_0\cdot\vec{M} \right\}, \tag{6}$$

with A_j the exchange constant of film (j). Thus, E_j includes exchange, demagnetizing, and Zeeman contributions (one needs to add also surface contributions that are relevant for the boundary conditions). The Landau-Lifshitz equation for the magnetization dynamics in film (j) is

$$\frac{d\vec{M}^j}{dt} = -|\gamma|_j\vec{M}^j \times \vec{H}_{\text{eff}}^j(\vec{M}), \tag{7}$$

with $|\gamma|_j$ the absolute value of the gyromagnetic factor of film (j), and the effective field $\vec{H}_{\text{eff}}^j(\vec{M}) = -\delta E_j/\delta\vec{M}$ is the sum of the applied, demagnetizing, and exchange fields acting at film (j):

$$\vec{H}_{\text{eff}}(\vec{M}) = H_0(\cos\theta_H\hat{z} + \sin\theta_H\hat{y}) + \vec{H}_D^j(\vec{M}) + \left(D_j/M_s^j\right)\nabla^2\vec{M}^j, \tag{8}$$

with D_j the exchange stiffness constant of film (j), $D_j = 2A_j/M_s^j$. Notice that the demagnetizing field $\vec{H}_D^j(\vec{M})$ in general has contributions from the magnetization of all the films (in the dynamic case), thus effectively coupling all the films. The linear approximation of the Landau-Lifshitz equations of motion follows from replacing Eq. (2) into Eq. (7), and then identifying the corresponding linear terms. Thus, the equation for the linear modes takes the following form in film (j):

$$i\omega\vec{m}_j^\omega = |\gamma|_j\hat{\tilde{z}}^j\left(D_j\nabla^2\vec{m}_j^\omega - M_s^j\nabla\phi_j^\omega - H_{\text{int}}^j\vec{m}_j^\omega\right), \tag{9}$$

with H_{int}^j the magnitude of the equilibrium internal field in film (j). We divide this equation by $4\pi M_s^j|\gamma_j|$, in which case it is written as

$$i\Omega_j\vec{m}_j^\omega = \hat{\tilde{z}}^j\left(d_j\nabla^2\vec{m}_j^\omega - \frac{1}{4\pi}\nabla\phi_j^\omega - h_{\text{int}}^j\vec{m}_j^\omega\right), \tag{10}$$

with $\Omega_j \equiv \omega/(4\pi M_s^j|\gamma_j|)$, $h_{\text{int}}^j \equiv H_{\text{int}}^j/(4\pi M_s^j)$ nondimensional frequencies and internal fields in film (j) (notice that the whole system oscillates with a single frequency ω, this is just notation), and $d_j = D_j/4\pi M_s^j = (l_{\text{ex}}^j)^2$ the square of the so called magnetostatic exchange length (dipolar length), which is a relevant length scale, that approximately indicates the length over which the spins are mainly aligned due to the strength of the exchange interaction relative to magnetostatic fields. In the case of a single film, Eq. (10) together with the finite thickness L of the film, indicate that the normalized frequencies of the modes Ω depend on the nondimensional ratios l_{ex}/L, h_{int} or H_{int}/M_s, and $l_{\text{ex}}\vec{Q}$, with $\vec{Q}$ the in-plane wave vector of the mode in question. In the case of several films the ratios between different gyromagnetic ratios, between magnetizations, and between exchange lengths, become also relevant variables in the determination of the modes dispersion relations and shapes.

B. Green-extinction equations

The frequencies of the spin wave modes as well as their amplitudes on the surfaces of the samples may be obtained by solving integral equations satisfied by them. These are homogeneous extinction equations that may be thought of as a generalization of Green's theorem to the equations relevant to this case, i.e., the magnetostatic equations and the Landau-Lifshitz equation. Integral equations are thus derived for the dipole-exchange normal modes evaluated on the surfaces of the multilayers.

1. Extinction equations outside magnetized films

Extinction equations can be derived for the normal modes of the system if one integrates in regions outside the magnetized samples the following expression that involves a so called auxiliary function [in this case represented by $\phi_0^{-\omega}(\vec{x} - \vec{x}')$, with $\vec{x}'$ an arbitrary reference point]. The latter satisfies the same magnetostatic equation in that region, as the modes, i.e., Eq. (4). The integrand is chosen as the following combination, and is null due to the first of Eqs. (3):

$$\int_{V_{\text{out}}} dV\,[\phi_0^{-\omega}(\vec{x} - \vec{x}')\boldsymbol{\nabla}\cdot\vec{b}^\omega(\vec{x}) - \phi^\omega(\vec{x})\boldsymbol{\nabla}\cdot\vec{b}_0^{-\omega}(\vec{x} - \vec{x}')] = 0. \tag{11}$$

The volume of integration is chosen outside magnetized samples, but ending on their limiting surfaces. Since $\vec{b}^\omega = -\boldsymbol{\nabla}\phi^\omega$ and $\vec{b}_0^{-\omega} = -\boldsymbol{\nabla}\phi_0^{-\omega}$, integrating by parts the previous equation one obtains

$$\int_S d\vec{S}\cdot[\phi_0^{-\omega}(\vec{x} - \vec{x}')\vec{b}^\omega(\vec{x}) - \phi^\omega(\vec{x})\vec{b}_0^{-\omega}(\vec{x} - \vec{x}')] = 0, \tag{12}$$

with S the surface of this nonmagnetized region, with its normal pointing outwards.

The previous equation involves a convolution over the z and x directions that in our model are in-plane unlimited coordinates associated with translational invariance. Since the Fourier transform of a convolution of two functions is the product of their Fourier transforms (evaluated with different signs of the wave vectors though), Eq. (12) leads to

$$0 = \phi_0^{-(\vec{Q},\omega)}(l_u - y')b_y^{(\vec{Q},\omega)}(l_u) - \phi^{(\vec{Q},\omega)}(l_u)b_{0y}^{-(\vec{Q},\omega)}(l_u - y') - \phi_0^{-(\vec{Q},\omega)}(l_d - y')b_y^{(\vec{Q},\omega)}(l_d) + \phi^{(\vec{Q},\omega)}(l_d)b_{0y}^{-(\vec{Q},\omega)}(l_d - y'), \tag{13}$$

here $\vec{Q}$ is the in-plane wave vector, and we have assumed that the outside nonmagnetized region lies between $y = l_d$ and $y = l_u$. Thus, conveniently the integral Eq. (12) have been transformed into the simple algebraic Eq. (13), at specific values of the wave vector $\vec{Q}$. Since Eq. (4) in Fourier space reads ($Q \equiv |\vec{Q}|$):

$$\partial^2\phi^\omega/\partial y^2 - Q^2\phi^\omega = 0, \tag{14}$$

we have $\phi_0^{-(\vec{Q},\omega)}(y-y') = \exp[\pm Q(y-y')]$, with $\pm$ representing two options of solutions. Using the previous two forms in Eq. (13) leads to the following two equations for the modes ($U \equiv l_u - l_d$ is the thickness of the nonmagnetized region in question, also notice that y' has played no role, it drops out of these equations):

$$\begin{pmatrix} e^{-QU} & -1 \\ 1 & -e^{-QU} \end{pmatrix}\begin{pmatrix} b_y^{(\vec{Q},\omega)}(l_u) \\ b_y^{(\vec{Q},\omega)}(l_d) \end{pmatrix} = Q\begin{pmatrix} e^{-QU} & -1 \\ -1 & e^{-QU} \end{pmatrix}\begin{pmatrix} \phi^{(\vec{Q},\omega)}(l_u) \\ \phi^{(\vec{Q},\omega)}(l_d) \end{pmatrix}. \tag{15}$$

These equations can be inverted, so that one may replace the unknowns $b_y^{(\vec{Q},\omega)}(l_u), b_y^{(\vec{Q},\omega)}(l_d)$ in terms of $\phi^{(\vec{Q},\omega)}(l_u), \phi(\vec{Q},\omega)(l_d)$:

$$\begin{pmatrix} b_y^{(\vec{Q},\omega)}(l_u) \\ b_y^{(\vec{Q},\omega)}(l_d) \end{pmatrix} = Q\begin{pmatrix} -\coth(QU) & \operatorname{csch}(QU) \\ -\operatorname{csch}(QU) & \coth(QU) \end{pmatrix}\begin{pmatrix} \phi^{(\vec{Q},\omega)}(l_u) \\ \phi^{(\vec{Q},\omega)}(l_d) \end{pmatrix}. \tag{16}$$

Notice that if one had exterior regions that extend to "infinity," the previous equations reduce to

$$b_y^{(\vec{Q},\omega)}(l_s) = Q\phi^{(\vec{Q},\omega)}(l_s), \tag{17}$$

$$b_y^{(\vec{Q},\omega)}(l_i) = -Q\phi^{(\vec{Q},\omega)}(l_i), \tag{18}$$

where $y = l_s, l_i$ represent the limiting surfaces of exterior regions extending to infinity in an upper and lower region, respectively. Equations (16)–(18) show that normal magnetic inductions at the surfaces may be replaced in terms of the magnetostatic potentials evaluated there.

2. *Extinction equations inside magnetized films*

In order to obtain extinction equations associated with the inside of magnetized samples, we consider the following integral over a magnetized sample volume:

$$\int_{V_{\text{in}}} dV[\phi^\omega(\vec{x})\nabla\cdot\vec{b}_I^{-\omega}(\vec{x}-\vec{x}') - \phi_I^{-\omega}(\vec{x}-\vec{x}')\nabla\cdot\vec{b}^\omega(\vec{x})] = 0, \tag{19}$$

with $\phi, \vec{b}$ corresponding to normal modes, and $\phi_I, \vec{b}_I$ representing auxiliary functions: both do satisfy the magnetostatic and Landau-Lifshitz equations, i.e., Eqs. (5) and (9) (but with different signs of the frequencies). The integrand is null due to the first of Eqs. (3) [notice that we have considered the auxiliary functions terms evaluated at $(-\omega)$, which will prove useful later; $\vec{x}'$ is a reference point]. Integrating by parts Eq. (19), one obtains

$$0 = \int_S d\vec{S}\cdot[\phi^\omega(\vec{x})\vec{b}_I^{-\omega}(\vec{x}-\vec{x}') - \phi_I^{-\omega}(\vec{x}-\vec{x}')\vec{b}^\omega(\vec{x})] - 4\pi\int_{V_{\text{in}}} dV[\nabla\phi^\omega(\vec{x})\cdot\vec{m}_I^{-\omega}(\vec{x}-\vec{x}') - \nabla\phi_I^{-\omega}(\vec{x}-\vec{x}')\cdot\vec{m}^\omega(\vec{x})], \tag{20}$$

Now, taking the cross product of Eq. (9) with $\vec{m}_I^{-\omega}$ and subtracting that of Eq. (9) evaluated for the auxiliary functions and at $(-\omega)$ with $\vec{m}^\omega$, one obtains

$$\nabla\phi^\omega(\vec{x})\cdot\vec{m}_I^{-\omega}(\vec{x}-\vec{x}') - \nabla\phi_I^{-\omega}(\vec{x}-\vec{x}')\cdot\vec{m}^\omega(\vec{x}) = \left(D_j/M_s^j\right)[\vec{m}_I^{-\omega}(\vec{x}-\vec{x}')\cdot\nabla^2\vec{m}^\omega(\vec{x}) - \vec{m}^\omega(\vec{x})\cdot\nabla^2\vec{m}_I^{-\omega}(\vec{x}-\vec{x}')]. \tag{21}$$

Using Eq. (21) in Eq. (20) and integrating by parts, one obtains the following extinction integral equation over the surface of the magnetized sample:

$$0 = \int_S d\vec{S}\cdot\left\{\phi^\omega(\vec{x})\vec{b}_I^{-\omega}(\vec{x}-\vec{x}') - \phi_I^{-\omega}(\vec{x}-\vec{x}')\vec{b}^\omega(\vec{x}) - 4\pi\left(D_j/M_s^j\right)\sum_{\tilde{k}}[m_{I\tilde{k}}^{-\omega}(\vec{x}-\vec{x}')\nabla m_{\tilde{k}}^\omega(\vec{x}) - m_{\tilde{k}}^\omega(\vec{x})\nabla m_{I\tilde{k}}^{-\omega}(\vec{x}-\vec{x}')]\right\}. \tag{22}$$

In the case of a thin film, which lies between $y = l_1$ and $y = l_2$, this previous extinction Eq. (22) corresponds to a convolution in the z and x directions in both surfaces of the sample, i.e., taking the Fourier transform of Eq. (22) in those directions, one transforms this integral equation into an algebraic equation for each independent value of the wave-vector $\vec{Q}$ and frequency ω:

$$\begin{aligned} 0 = {} & b_y^I(l_2-y')\phi(l_2) - \phi^I(l_2-y')b_y(l_2) - b_y^I(l_1-y')\phi(l_1) + \phi^I(l_1-y')b_y(l_1) \\ & - \frac{d_j}{2}\left(\frac{\partial M_-}{\partial y}(l_2)M_+^I(l_2-y') + \frac{\partial M_+}{\partial y}(l_2)M_-^I(l_2-y') - \frac{\partial M_-}{\partial y}(l_1)M_+^I(l_1-y') - \frac{\partial M_+}{\partial y}(l_1)M_-^I(l_1-y')\right) \\ & + \frac{d_j}{2}\left(\frac{\partial M_-^I}{\partial y}(l_2-y')M_+(l_2) + \frac{\partial M_+^I}{\partial y}(l_2-y')M_-(l_2) - \frac{\partial M_-^I}{\partial y}(l_1-y')M_+(l_1) - \frac{\partial M_+^I}{\partial y}(l_1-y')M_-(l_1)\right), \end{aligned} \tag{23}$$

where we have simplified notation by excluding labels $(\vec{Q},\omega)$ for the modes and $-(\vec{Q},\omega)$ for the auxiliary functions [$M_\pm \equiv 4\pi(m_x \pm i m_y)$ and $d_j \equiv D_j/4\pi M_s^j$]. In Appendix A 1 the following auxiliary functions of exponential form are determined:

$$\phi_I^{-(\vec{Q},\omega)} = Ae^{-\alpha(y-y')}, \quad M_\pm^I = B_\pm e^{-\alpha(y-y')}, \tag{24}$$

i.e.,

$$b_y^I = [\alpha A - i(B_+ - B_-)\cos\theta_M/2]\exp[-\alpha(y-y')]. \tag{25}$$

There are six different auxiliary solutions associated with each film (j), i.e., $\alpha = \alpha_n^{(j)}$ with $n = 1,\ldots,6$, and with associated coefficients $A_n^{(j)}$, $B_\pm^{n(j)}$, see Appendix A 1 for details. The α's are solutions of a sixth order equation, Eq. (A6). Using Eqs. (24) and (25) in Eq. (23), one obtains the following set of six extinction equations ($n = 1,\ldots,6$) associated with film (j) for the modes of wave vector $\vec{Q}$:

$$\begin{aligned} 0 = {} & e^{-\alpha L}\{[\alpha A - i(B_+ - B_-)\cos\theta_M/2]\phi(l_2) - Ab_y(l_2)\} + Ab_y(l_1) - [\alpha A - i(B_+ - B_-)\cos\theta_M/2]\phi(l_1) \\ & - (d/2)e^{-\alpha L}\{[M'_+(l_2) + \alpha M_+(l_2)]B_- + [M'_-(l_2) + \alpha M_-(l_2)]B_+\} \\ & + (d/2)\{[M'_+(l_1) + \alpha M_+(l_1)]B_- + [M'_-(l_1) + \alpha M_-(l_1)]B_+\}, \end{aligned} \tag{26}$$

where indices (j) and n indicating film (j) and solution n (from $\alpha_n^{(j)}$) are not shown for simplicity; $M'_\pm$ is shorthand for $\partial M_\pm/\partial y$, and $L = l_2 - l_1$ is the thickness of film (j).

In Sec. IV on boundary conditions, it is shown that for different mechanisms operating at the surfaces it is possible to express the values of the normal derivatives of the magnetization at the different surfaces, i.e., the $M'_\pm(l_j)$'s, in terms of the magnetization components at the surfaces, i.e., the $M_\pm(l_n)$'s, and proceed to solve then the extinction equations with as many equations as unknowns. This is explained in the following section.

Now, if one defines for each film the nondimensional quantities $\tilde{\alpha} \equiv \alpha l_{\rm ex}$, $\tilde{Q} = Ql_{\rm ex}$, $\tilde{k} = kl_{\rm ex}$, $\tilde{q} = ql_{\rm ex}$, then Eq. (A6) for α written in terms of nondimensional variables reads (without indices j, n)

$$2(\tilde{\alpha}^2 - \tilde{Q}^2) = -[(\tilde{k}\sin\theta_M + i\tilde{\alpha}\cos\theta_M)^2 + \tilde{q}^2]\left(\frac{1}{\tilde{\alpha}^2 - \tilde{Q}^2 - h_{\rm int} + \Omega} + \frac{1}{\tilde{\alpha}^2 - \tilde{Q}^2 - h_{\rm int} - \Omega}\right), \tag{27}$$

i.e., $\tilde{\alpha}$ is a function of the nondimensional variables $\vec{\tilde{Q}}$, H_0/M_s, and Ω.

Now, if these nondimensional quantities just defined are used in Eq. (26), it reads

$$\begin{aligned} 0 = {} & e^{-\tilde{\alpha}\tilde{L}}\{[2\tilde{\alpha} - (\tilde{b}_+ - \tilde{b}_-)\cos\theta_M]\phi(l_2) - 2b_y(l_2)\} + 2b_y(l_1) - [2\tilde{\alpha} - (\tilde{b}_+ - \tilde{b}_-)\cos\theta_M]\phi(l_1) \\ & - e^{-\tilde{\alpha}\tilde{L}}\{[\tilde{M}'_+(l_2) + \tilde{\alpha}\tilde{M}_+(l_2)]\tilde{b}_- + [\tilde{M}'_-(l_2) + \tilde{\alpha}\tilde{M}_-(l_2)]\tilde{b}_+\} + [\tilde{M}'_+(l_1) + \tilde{\alpha}\tilde{M}_+(l_1)]\tilde{b}_- + [\tilde{M}'_-(l_1) + \tilde{\alpha}\tilde{M}_-(l_1)]\tilde{b}_+, \end{aligned} \tag{28}$$

with $\tilde{L} \equiv L/l_{\rm ex}$, $B_\pm = -iAb_\pm$ ($\tilde{b}_\pm$ depend on the same variables as $\tilde{\alpha}$), $\tilde{M}_\pm \equiv -id M_\pm$. Equation (28) plus the replacement of the boundary conditions (as just explained) shows explicitly the dependence of the modes on the nondimensional variables $\tilde{L} \equiv L/l_{\rm ex}^j$, H_0/M_s^j, $\vec{\tilde{Q}}$ and on the gyromagnetic ratios $|\gamma_j|$, as predicted after the Landau-Lifshitz Eq. (10).

3. Set of extinction equations for multiple films

In the previous two sections we wrote extinction equations for generic regions that are nonmagnetized or that correspond to magnetized films. The unknowns in these equations are physical variables evaluated at the edges or surfaces of these regions: the magnetostatic potential, the normal magnetic induction, the normal derivative of magnetization components, and magnetization components (the frequency is also an unknown, which ultimately is the eigenfrequency of a normal mode). More specifically, the unknowns are Fourier components of these variables that do not couple to other Fourier components due to in-plane translational invariance.

In the following we discuss how these equations are solved if there are multiple films. For this it is better to understand first the case of a single film [37]: Eq. (26) corresponds to six equations (six possible values of α) for 12 unknowns [$M_\pm(l_u)$, $M_\pm(l_d)$, $M'_\pm(l_u)$, $M'_\pm(l_d)$, $\phi(l_u)$, $\phi(l_d)$, $b_y(l_u)$, $b_y(l_d)$]. The boundary conditions associated with the exchange interaction (to be detailed in another section) relate the normal derivatives of the magnetization to the magnetization components at the surfaces, thus reducing the number of unknowns by four. Furthermore, Eqs. (17) and (18) correspond to the regions over and under the film, and as explained before allow us to reduce by two the number of unknowns. Thus, at the end one has effectively the six homogeneous equations, Eq. (26), for six unknowns [$M_\pm(l_u)$, $M_\pm(l_d)$, $\phi(l_u)$, $\phi(l_d)$], with the frequency as an unknown also: this is a well posed eigenvalue problem for the frequency of the modes and their shapes at the surfaces of the film (these linear modes are arbitrary up to a multiplicative constant).

Now, every time an extra film is added to the system, there are effectively six more equations and six more unknowns on the surfaces of the films, i.e., the problem remains well posed and with a reasonable size. Indeed a new film represents six more equations of the type of Eq. (26), with 12 more unknowns, but four of those are eliminated by the exchange boundary conditions and another two of those are effectively eliminated by the two extra Eq. (16) that correspond to a new interfilms region. An important point that was implicitly used

in the previous analysis is that the magnetostatic boundary conditions correspond to both continuous normal magnetic induction and magnetostatic potential, which means that the unknowns in the equations outside the films are the same as the analogous ones in the inside equations, i.e., the outside equations do not add extra unknowns.

4. Spin wave modes everywhere

If one is interested in determining the value of all the physical variables everywhere, i.e., inside magnetized films or outside them, the presented method in terms of extinction equations using auxiliary functions may be extended to do this. First, if one is interested in determining the magnetostatic potential in a nonmagnetized region, one may use Eq. (12) where the cross section of the volume of integration that leads to this equation corresponds to a rectangular section that has as one edge the surface of a film ($y = l_d$ in the previous notation) and the other edge is at level y inside this nonmagnetized region. Thus, the equivalent of Eq. (15) becomes in this case

$$\begin{pmatrix} -Qe^{-Q(y-l_d)} & e^{-Q(y-l_d)} \\ Q & 1 \end{pmatrix} \begin{pmatrix} \phi^{(\vec{Q},\omega)}(y) \\ b_y^{(\vec{Q},\omega)}(y) \end{pmatrix} = \begin{pmatrix} -Q & 1 \\ Qe^{-Q(y-l_d)} & e^{-Q(y-l_d)} \end{pmatrix} \begin{pmatrix} \phi^{(\vec{Q},\omega)}(l_d) \\ b_y^{(\vec{Q},\omega)}(l_d) \end{pmatrix}, \tag{29}$$

which can be inverted to give

$$\begin{pmatrix} \phi^{(\vec{Q},\omega)}(y) \\ b_y^{(\vec{Q},\omega)}(y) \end{pmatrix} = \begin{pmatrix} \cosh[Q(y-l_d)] & -\sinh[Q(y-l_d)]/Q \\ -Q\sinh[Q(y-l_d)] & \cosh[Q(y-l_d)] \end{pmatrix} \begin{pmatrix} \phi^{(\vec{Q},\omega)}(l_d) \\ b_y^{(\vec{Q},\omega)}(l_d) \end{pmatrix}. \tag{30}$$

Thus one has obtained expressions for $\phi^{(\vec{Q},\omega)}(y)$, $b_y^{(\vec{Q},\omega)}(y)$, i.e., the fields inside nonmagnetized regions, in terms of the known values of $b_y^{(\vec{Q},\omega)}(l_d)$, $\phi^{(\vec{Q},\omega)}(l_d)$ at the surface of a contiguous film.

Furthermore, if one is interested in the physical variables inside a magnetized region, using an analogous procedure leads to the following equations, where y is a level inside the magnetized region (j):

$$\begin{aligned} 0 = {} & e^{-\alpha(y-l_1)}\{[\alpha A - i(B_+ - B_-)\cos\theta_M/2]\phi(y) - Ab_y(y)\} + Ab_y(l_1) - [\alpha A - i(B_+ - B_-)\cos\theta_M/2]\phi(l_1) \\ & - (d/2)e^{-\alpha L}\{[M'_+(y) + \alpha M_+(y)]B_- + [M'_-(y) + \alpha M_-(y)]B_+\} + (d/2)\{[M'_+(l_1) + \alpha M_+(l_1)]B_- + [M'_-(l_1) + \alpha M_-(l_1)]B_+\}. \end{aligned} \tag{31}$$

These are six inhomogeneous equations (associated to six different α) for six unknowns, i.e., $b_y(y)$, $\phi(y)$, $M'_+(y)$, $M_+(y)$, $M'_-(y)$, $M_-(y)$, that can be solved with ease for these physical variables since it is a 6×6 system of linear equations [the variables evaluated at the surface $y = l_1$ were determined previously from the solution to the eigensystem of equations associated with Eq. (26)].

III. SYMMETRIC STACKS OF FILMS, MODES WITH RECIPROCAL AND NONRECIPROCAL FEATURES

In the case of a stack of films that is symmetric with respect to reflections with respect to a given central plane, modes that propagate in opposite directions (or whose in-plane wave vectors differ only by their signs) have the same frequencies, i.e., reciprocal with respect to frequencies, and have shapes that are related but nonreciprocal (their respective magnetostatic potential and magnetization components are symmetric or antisymmetric specular reflections of each other with respect to the central symmetry plane). This property is independent of the angle in which the magnetic dc field is applied to the structure, and it is valid both for magnetostatic and dipole-exchange modes.

The previous reciprocal and nonreciprocal properties under change of sign of the wave vector may be deduced directly from the structure of the extinction equations in wave vector space. Notice that in their final form these equations include the boundary conditions. The details of this are presented in Appendix A 3 a, where the eigenvalue equations for the modes and their frequencies are analyzed with respect to how their solutions differ under a change of sign of the wave vector. This is done for magnetostatic as well as for dipole-exchange modes.

The underlying symmetry that explains these properties under the change of sign of the wave vector is that for a symmetric stack of films if one applies the dc magnetic field in the opposite direction and analyzes the modes with respect to inverted axis (centered in the symmetry plane) the problem becomes equivalent to the original one. This means that the original modes should be also modes of the case with inverted dc magnetic field and inverted axis of reference, but these modes are written with respect to the new reference frame and in the new coordinates. The equations for these modes may be retraced to the original coordinates and in the process one discovers that there are modes for the original system, i.e., with nonreversed magnetic field, that have the same frequencies of the original modes, but whose magnetostatic potentials and magnetization components are symmetric and antisymmetric specular reflections of the respective fields of the original modes. This is explained in more detail in Appendix A 3 b.

IV. BOUNDARY CONDITIONS

We are using a micromagnetic continuous model in order to determine the dipole-exchange spin wave modes of multilayered structures. Within this model one needs to impose magnetostatic boundary conditions, i.e., the continuity of normal magnetic induction and of magnetostatic potential

(these are sufficient for magnetostatic modes), but also the introduction of the exchange field, which involves second order partial derivatives, requiring the consideration of supplemental boundary conditions at the surfaces of the films. In the following we briefly review work presented in several references on this issue of nonmagnetostatic boundary conditions within the continuum model.

A relevant initial work on the topic corresponds to that of Rado and Weertman in Ref. [19] that introduces the concept of general "exchange boundary conditions," through writing the Landau-Lifshitz equation of motion for the magnetization of a ferromagnet as

$$-(1/|\gamma|)\partial\vec{M}/\partial t = \left(2A/M_s^2\right)\vec{M}\times\nabla^2\vec{M} + \vec{T}_{\rm vol}, \tag{32}$$

i.e., the torque on the magnetization is separated into an exchange part plus all the extra volumetric terms $\vec{T}_{\rm vol}$. Then the idea was to integrate the previous expression over a small volume V that covers the region of separation of the ferromagnet from the outside (for the moment assumed nonmagnetic), leading to

$$0 = -\left(2A/M_s^2\right)\int_S dS\vec{M}\times(\partial\vec{M}/\partial n) + \int dS\vec{T}_{\rm sup}, \tag{33}$$

where the first term represents a superficial torque of exchange origin (it is explained in Appendix A 4 a, n represents a normal direction to the sample surface, pointing to the exterior of it), and $\vec{T}_{\rm sup}$ represents a torque per unit surface area with contribution from concentrated superficial torques, which may have different physical origins.

One of the possible sources of $\vec{T}_{\rm sup}$ corresponds to surface anisotropies. For example, a form of surface anisotropy areal energy density is $U_{\rm an}^s = K_s[1-(\vec{M}\cdot\vec{n}/M_s)^2]$ ($\hat{n}$ is the unitary vector normal to the surface, pointing to the exterior of the sample). For a film with uniaxial surface anisotropy Soohoo [20] derived the following form of the boundary conditions for the dynamic magnetization components, which include partial pinning (in our case the sign of K_s differs from that reference):

$$0 = \frac{\partial m_{\tilde{y}}}{\partial n} - \lambda\cos(2\theta_M)m_{\tilde{y}}, \tag{34}$$

$$0 = \frac{\partial m_x}{\partial n} + \lambda\sin^2(\theta_M)m_x, \tag{35}$$

with $\lambda = K_s/A$ (see also Ref. [42]), $n = y$ in the upper surface of a film, and $n = -y$ in the lower one, θ_M is the angle that the equilibrium magnetization makes with the plane of the film. We refer to Eqs. (34) and (35) as the partially pinned boundary conditions, which are derived in Appendix A 4 b. Equations (34) and (35) correspond to an application of Eq. (33), they are their dynamic linear version (in the case of a magnetic field applied obliquely they are approximate since the equilibrium magnetization configuration is also approximate, and they were used for example in Ref. [4]).

Another source of $\vec{T}_{\rm sup}$ corresponds to the case of an effective pinning if the ferromagnet is in contact with an antiferromagnet, the exchange-bias effect [43]. In this case there is an exchange interaction between the interfacial layers of the ferromagnet and the antiferromagnet, which is simply modeled [43] via a surface energy:

$$U_S = \vec{p}\cdot\vec{M}, \tag{36}$$

with p a pinning parameter, and $-\vec{p}$ an effective exchange bias field. Thus, in this model it follows that

$$\vec{T}_{\rm sup} = -\vec{M}\times\vec{p}. \tag{37}$$

More recently, a boundary condition resulting from a ferromagnet that has interfacial Dzyaloshinskii-Moriya interaction (IDMI), has been discussed in Ref. [44]. In this case $\vec{T}_{\rm sup}$ is modeled as

$$\vec{T}_{\rm sup} = \int_{L-b}^{L} dy\vec{M}\times\vec{H}_{\rm sup}, \tag{38}$$

with L the thickness of the film, b the thickness of the interface atomic layer, and the interface effective magnetic field originating from IDMI is given by

$$\vec{H}_{\rm sup} = -(2\tilde{D}/M_s)\hat{z}\times\partial\vec{m}/\partial x, \tag{39}$$

with $\tilde{D}$ a Dzyaloshinskii-Moriya constant, and $\hat{z}$ the in-plane direction of an applied magnetic field (direction of the equilibrium magnetization also). In the case of a Damon-Eshbach surface mode studied in Ref. [44], with wavevector k [$\exp(-ikx)$ dependence], the previous surface torque becomes

$$\vec{T}_{\rm sup} = -2i\tilde{D}bk[m_x\hat{x} + m_y\hat{y}]. \tag{40}$$

Substitution into Eq. (33) leads to equations for the dynamic magnetization components of the type

$$0 = \partial m_y/\partial y - \frac{i\tilde{D}kb}{A}m_x, \tag{41}$$

$$0 = \partial m_x/\partial y + \frac{i\tilde{D}kb}{A}m_y, \tag{42}$$

for an upper surface.

The final type of boundary condition (BC) that we discuss is related to the direct exchange interfacial interaction between two ferromagnetic layers, something that has been discussed in several references [21–26]. Initial works on the topic were those of Hoffmann *et al.* [21,22], where effective boundary conditions between two ferromagnetic layers were derived using a semiclassical model of exchange coupling. Those boundary conditions were reconsidered by several authors [23–26] since the Hoffmann BCs do not have a proper behavior in the limit of a single continuous film. The resulting Barnas-Mills boundary conditions [25,26] overcame those difficulties. Although these BC may be derived semiclassically starting from a Heisenberg model for the exchange, they also may be derived assuming that there is an interfacial energy written within a continuum approach, as follows:

$$E_{\rm sup} = -\int dyA_{12}\delta(y)\vec{M}_1(-a/2)\cdot\vec{M}_2(a/2), \tag{43}$$

with y the normal coordinate, and the lattice planes of both materials are located at $y = \pm a/2$. The associated surface torque acting on the lower surface ($y = -a/2$) is

$$\vec{T}_{\rm sup} = A_{12}\vec{M}_1(-a/2)\times\vec{M}_2(a/2), \tag{44}$$

while in the upper surface the torque is the negative of the previous one.

Actually, in the case of the continuum model, locating effectively the interface at $y = 0$ solved the inconsistencies

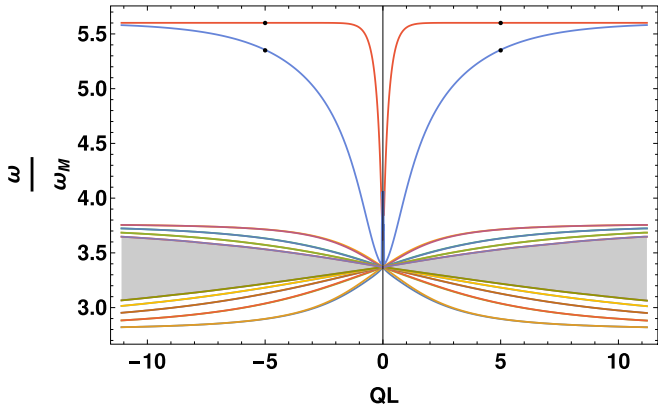

FIG. 3. Dispersion relations of magnetostatic modes of a ferromagnetic bilayer made of equivalent films. The films are separated by 20% of the thickness L of each film. Applied magnetic field of magnitude $H_0 = 6.4M_s$ at an oblique angle $\theta_H = 0.454\pi$, $\theta_M = 0.154\pi$, $\varphi = 0.3\pi$ (in the figure negative wave vectors correspond to $\varphi = 0.3\pi + \pi$. Internal field $H_i = 1.04M_s$, $\omega_M \equiv |\gamma|M_s$, Q is the in-plane wave vector in the ϕ direction.

present in the initial Hoffmann model. The dynamics of the magnetization at the interfacial lattice planes that follows from Eq. (43) leads to the following Barnas-Mills boundary conditions [25,26,45]:

$$0 = A_{12}\vec{M}_2^{0+} \times \vec{M}_1^{0-} + \frac{a}{2}A_{12}\left(\frac{\partial \vec{M}_2^{0+}}{\partial y} \times \vec{M}_1^{0-} + \frac{\partial \vec{M}_1^{0-}}{\partial y} \times \vec{M}_2^{0+}\right) + \frac{A_1}{M_1^2}\left(\vec{M}_1 \times \frac{\partial \vec{M}_1}{\partial y}\right)_{0-} + \frac{A_2}{M_2^2}\left(\vec{M}_2 \times \frac{\partial \vec{M}_2}{\partial y}\right)_{0+}, \quad (45)$$

$$0 = \frac{A_2}{M_2^2}\left(\vec{M}_2 \times \frac{\partial \vec{M}_2}{\partial y}\right)_{0+} - \frac{A_1}{M_1^2}\left(\vec{M}_1 \times \frac{\partial \vec{M}_1}{\partial y}\right)_{0-}. \quad (46)$$

In Appendix A 4 c the Barnas-Mills boundary conditions [Eqs. (45) and (46)] are derived and their linear version is presented (they contain approximations for magnetic fields applied in oblique directions, of similar origin as in the case of surface anisotropy boundary conditions). Notice that in Ref. [45] boundary conditions at ferromagnetic interfaces of finite thickness have been discussed, and it also contains a discussion of most of the boundary conditions previously mentioned.

V. EXAMPLES OF MAGNETOSTATIC AND DIPOLE-EXCHANGE MODES IN FERROMAGNETIC FILMS

A. Magnetostatic modes in films

In the following we present specific examples of magnetostatic modes calculations. In Appendix A 2 we discuss how the magnetostatic modes are determined within the context of the application of the extinction-Green theorems: it is much simpler than for dipole-exchange modes, since there are only two eigenvalue equations per film. We write the in-plane wave vector as $\vec{Q} = q\hat{x} + k\hat{z} = Q(\sin\varphi\hat{x} + \cos\varphi\hat{z})$, and in following figures negative wave vectors means $\varphi \to \varphi + \pi$.

First, we consider two films of equal characteristics, separated by a distance that is 20% of the thickness of each film (L), there is a magnetic field of magnitude $H_0 = 6.4M_s$ applied at an angle $\theta = 0.454\pi$ from the plane: this leads to an internal field of magnitude $1.04M_s$ and inclination angles of the magnetization $\theta_M = 0.154\pi$ in each film. Also $\varphi = 0.3\pi$. For this symmetric bilayer we present in Fig. 3 the dispersion relations for negative and positive wave vectors: frequency reciprocity with respect to the sign of the wave vector is evidenced. These results correspond to similar parameters to the system presented in the dipole-exchange case of Fig. 6 of Ref. [11] (we selected the parameters such that the internal field would be approximately equal to M_s in magnitude). In Fig. 3 one sees several lower frequency "volume" modes with characteristics analogous to those discussed for a single film in Ref. [37], which in the case of a magnetic field applied at an oblique angle show forward and backward characteristics; and a couple of "surface" modes of higher frequencies (the continuous dark region in the "volume" modes region represents many modes with close frequencies). Then, Fig. 4 shows plots of the magnetostatic potential at specific values of the wave vector for the just mentioned two surface modes: one sees that although there is frequency reciprocity for this pair of equal films, there is nonreciprocity with respect to the shapes of the modes (the specific values of Q and ω at which these modes are plotted are marked with points in Fig. 3). It is known that this mode nonreciprocity exists for single films [41], i.e., that for a given sign of the wave vector or direction of propagation the surface mode propagates, located on one surface of the film, while for the other sign it travels bound to the opposite surface. In this case we have a couple of ferromagnetic films that are close and with an almost perpendicularly applied magnetic field. Figures 4(a) and 4(b) correspond to the higher

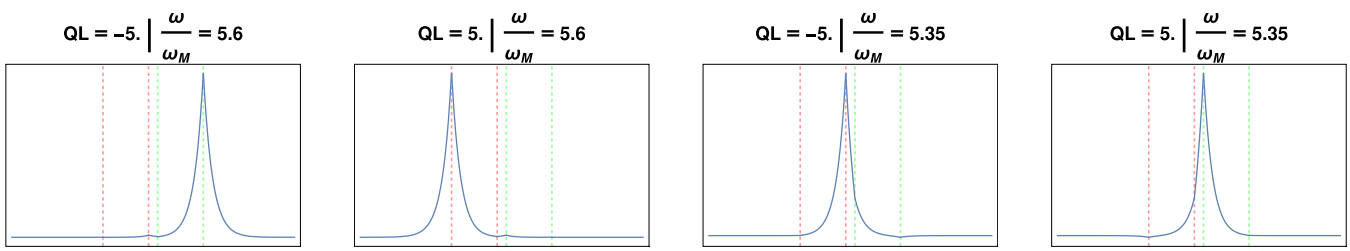

FIG. 4. Magnetostatic potential of magnetostatic modes of a bilayer of ferromagnetic material. Films are separated by 20% of the thickness L of each film. Applied magnetic field at an oblique angle $\theta = 0.454\pi$, of magnitude $H_0 = 6.4M_s$, $\theta = 0.454\pi$, $\theta_M = 0.154\pi$, $\varphi = 0.3\pi$.

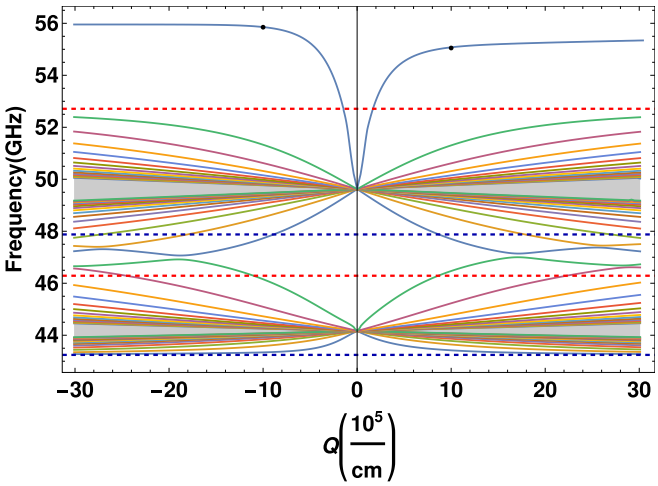

FIG. 5. Dispersion relations of magnetostatic modes of a bilayer of Ni and Fe. The films are separated by 6 Å, and have equal thicknesses $L_{\rm Fe} = L_{\rm Ni} = 200$ Å. Applied magnetic field at an oblique angle $\theta_H = 0.3\pi$, of magnitude $H_0 = 15.9$ kG, $\theta_{\rm Fe} = 0.135\pi$, $\theta_{\rm Ni} = 0.24\pi$, $\varphi = 0.35\pi$. Internal fields $H^i_{\rm Fe} = 10.26$ kG, $H^i_{\rm Ni} = 12.81$ kG.

frequency surface mode and different signs of the wave vector, they may be understood in terms that the surface modes are located at the outer surfaces of the two different films, i.e., effectively on the opposite sides but also far apart. While for the lower frequency surface mode and again for different signs of the wave vector Figs. 4(c) and 4(d) show the surface modes in different films and effectively opposite sides, but in this case the modes have significant amplitudes in the opposite film, explaining the frequency difference with the modes of Figs. 4(a) and 4(b).

In Fig. 5 we present magnetostatic dispersion relations for a bilayer of different ferromagnets, Ni and Fe films. There is a magnetic field of magnitude $H_0 = 15.9$ kG applied at an oblique angle $\theta_H = 0.3\pi$, the films are separated by a distance of 6 Å, each has a thickness of $L_{\rm Fe} = L_{\rm Ni} = 200$ Å, and $\varphi = 0.35\pi$. The main features of the dispersion relations are associated with the features of isolated modes in each film [37]. For example, we see dispersion relations emerging at $Q = 0$ from frequencies close to 44 and 50 GHz, while according to the theory of a single film [37] they should emerge at $\omega = |\gamma|\sqrt{H_i^2 + H_i \cos^2\theta_M}$, with H_i the internal field inside the respective film, which leads to values of 44.1 and 49.6 GHz, respectively, for Ni and Fe, i.e., there is coincidence (values for parameters of Ni and Fe were taken as in Fig. 9 of Ref. [17], i.e., for Ni $4\pi M_s = 6$ kG, $g = 2.2$ and for Fe $4\pi M_s = 21$ kG, $g = 2.1$). Furthermore, according to Ref. [37], for a single film volume modes frequencies should lie in the range between $\omega = |\gamma|\sqrt{H_i^2 + 4\pi M_s H_i \sin^2\varphi \cos^2\theta_M}$ and $\omega = |\gamma|\sqrt{H_i^2 + 4\pi M_s H_i}$, which is broadly consistent with Fig. 5, since $H_i^{\rm Ni} = 12.81$ kG, $\theta_{\rm Ni} = 0.24\pi$, and $H_i^{\rm Fe} = 10.26$ kG, $\theta_{\rm Fe} = 0.135\pi$. These previous frequency limits are represented for each film by dashed horizontal lines in Fig. 5, of different colors, notice that there is an overlap between volume modes frequencies. In particular one sees that in this case there is frequency nonreciprocity for the surface modes as the sign of the wave vector is changed.

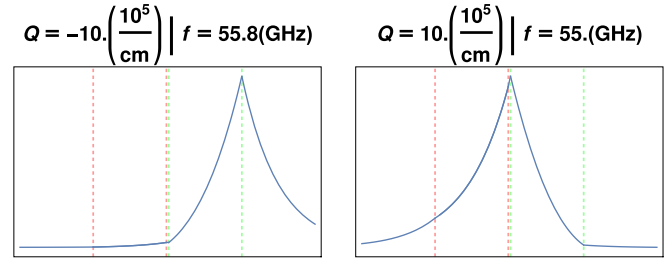

FIG. 6. Magnetostatic potential of magnetostatic surface modes of a bilayer of Ni and Fe, at particular values of frequencies and wave vectors ($\omega = 55.8$ GHz, $Q = \pm 10^6$/cm). The films are separated by 6 Å, and have equal thicknesses $L_{\rm Fe} = L_{\rm Ni} = 200$ Å. Applied magnetic field of magnitude $H_0 = 15.9$ kG at an oblique angle $\theta = 0.3\pi$, $\theta_{\rm Fe} = 0.135\pi$, $\theta_{\rm Ni} = 0.24\pi$, $\varphi = 0.35\pi$.

The higher frequency modes of Fig. 5 (blue lines) are surface modes localized mainly in the Fe film, and in this case have different frequencies for different signs of the wave vector due to the interaction with the Ni film. As mentioned, the highest frequency volume modes of isolated Ni have an overlap with the lowest volume modes of isolated Fe, and this leads to hybridization between these modes when the films are close together, as is evident in the region around 47 GHz. Figure 6 shows plots of the magnetostatic potential of the highest surface modes just mentioned (originating in Fe), at particular values of the wave vectors (the frequencies and wave vectors of these plots are marked by dots in Fig. 5). Figure 6(a) corresponds to a negative wave vector, it shows the magnetostatic potential of a mode of surface character that is mainly confined to the exterior surface of the Fe film; and Fig. 6(b) corresponds to a surface mode with a positive wave vector of the same magnitude, the magnetostatic potential is mainly confined to the interior surface of the Fe film, but in

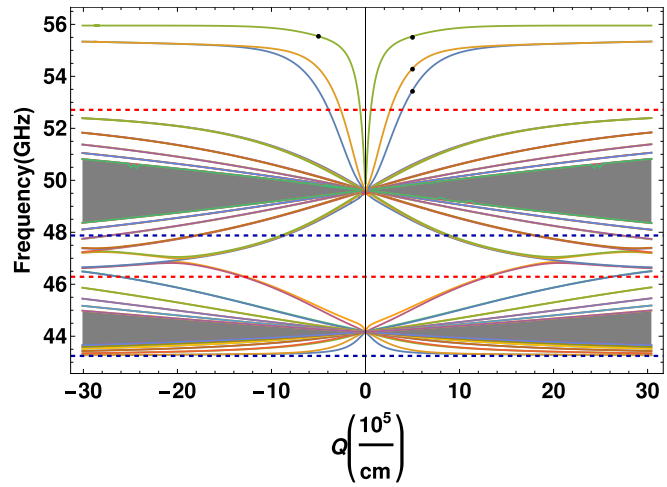

FIG. 7. Dispersion relations of magnetostatic modes of a multilayer of Ni (two films) and Fe (three films) symmetrically located, as in Fig. 1. The films are separated by 6 Å, and have equal thicknesses $L_{\rm Fe} = L_{\rm Ni} = 200$ Å. Applied magnetic field of magnitude $H_0 = 15.9$ kG at an oblique angle $\theta_H = 0.3\pi$, $\theta_{\rm Fe} = 0.135\pi$, $\theta_{\rm Ni} = 0.24\pi$, $\varphi = 0.35\pi$. Internal fields $H^i_{\rm Fe} = 10.26$ kG, $H^i_{\rm Ni} = 12.81$ kG.

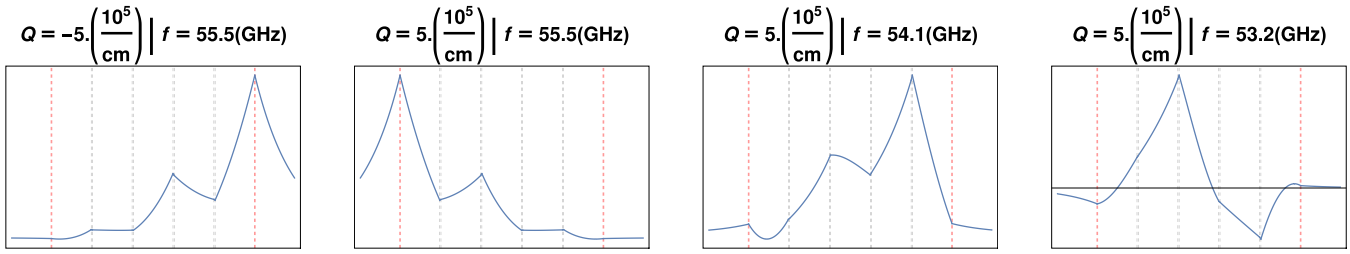

FIG. 8. Magnetostatic potential of magnetostatic surface modes of a a multilayer of Ni (two films) and Fe (three films). Same parameters as in Fig. 7, and plots correspond to marked points there. (a) and (b) Correspond to the highest frequency surface mode, with wave vectors $\pm 5 \times 10^5/\mathrm{cm}$, and (c) and (d) to the lower frequency surface modes at $Q = +5 \times 10^{-5}/\mathrm{cm}^2$.

this case it has also significant values inside Ni, explaining why its frequency differs from that of mode (a).

We now include Figs. 7 and 8 that correspond to magnetostatic modes of a multilayer of five films, two of Ni, and three of Fe (intercalated and ordered in a symmetrical way, as in Fig. 1). Figure 7 shows the dispersion relations of the magnetostatic modes, its interpretation is similar to the one given for the case of a bilayer of Ni and Fe of Fig. 5: one still has frequency reciprocity under change of wave-vector sign, although in this case there are more modes since there are more coupled films. And Fig. 8 shows plots of the magnetostatic potential in particular cases: those of the surface modes marked by points in Fig. 7. We included this figure in order to show that these surface modes may have significant amplitudes in almost all of the films involved. In particular, Figs. 8(a) and 8(b) correspond to the highest frequency surface mode, with wave vectors that are the negative of each other ($Q = 5 \times 10^{-5}/\mathrm{cm}^2$): one sees that there is nonreciprocity of the mode shapes in this case, but evidently they do have a reflection symmetry with respect to each other. Furthermore, Figs. 8(c) and 8(d) show the magnetostatic potential of the lower frequency surface modes for the same and positive wave vector: again one sees important amplitudes of the potential in almost all films, but with a different distribution.

B. Dipole-exchange modes in films

In the following we discuss results on dipole-exchange modes that follow from the application of the theory presented in the previous sections.

As a first example, we consider a bilayer made of two equivalent ferromagnetic films, with exchange constant such that $A/L^2 = 0.1$, with L the thickness of one film. In Fig. 9(a) a comparison is made of dipole-exchange dispersion relations of this bilayer between the cases magnetized in-plane with longitudinal ($\varphi = 0$, dashed curves) and perpendicular propagation ($\varphi = \pi/2$) that correspond to the left figure (actually this figure reproduces the results of Fig. 6 of Ref. [11], except that we have included results for negative wave vectors), with those of the right figure that correspond to the bilayer magnetized obliquely, with an equivalent internal field (in magnitude) to the previous cases and with $\varphi = 0.3\pi$. In the right figure we also compare the dipole-exchange modes frequencies with the corresponding magnetostatic modes frequencies (dashed curves) for the same parameters: the coincidence is good at low values of the in-plane wave vectors, as expected. This allows us to understand the structure of the dipole-exchange modes at low wave vectors, since the figure shows clearly hybridization between surface modes of magnetostatic origin with exchange dominated modes. As for magnetostatic modes in bilayers of identical

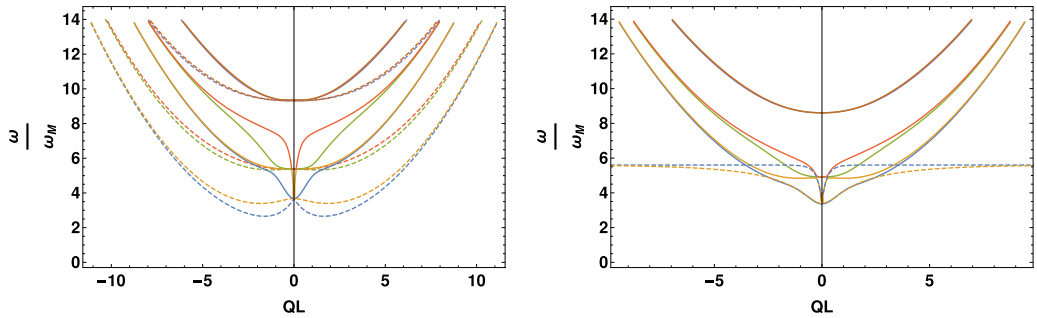

FIG. 9. Dispersion relations of dipole-exchange modes of a double layer made of equivalent ferromagnetic films, with an exchange A constant such that $A/L^2 = 0.1$, with L the thickness of a single film, Q the wave vector, $\omega_M \equiv |\gamma| M_s$. Left figure: Magnetic field applied in-plane, of magnitude $H_0 = M_s$, dashed curves correspond to $\varphi = 0$, and continuous curves to $\varphi = \pi/2$. Right figure: Magnetic field applied at an oblique angle $\theta = 0.454\pi$, of magnitude $H_0 = 6.4 M_s$, $\theta_M = 0.154\pi$, $\varphi = 0.3\pi$, internal field of magnitude $H_i^{\mathrm{Fe}} = 1.04 M_s$. This figure includes comparison with pure magnetostatic modes dispersion relations for low values of the wave-vector Q, which are the dashed curves.

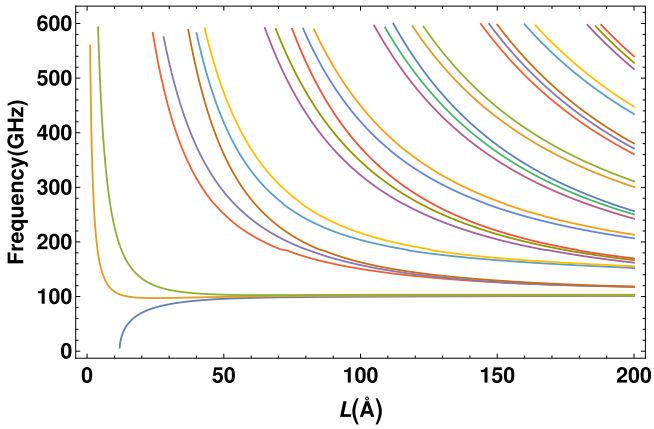

FIG. 10. Frequencies of dipole-exchange modes of a multilayer stack Fe/Ni/Fe/Ni/Fe, as a function of the common thickness L of each layer. Applied magnetic field of magnitude $H_0 = 16.94$ kG at an oblique angle $\theta = 0.49\pi$, $\theta_{\rm Fe} = 0.28\pi$, $\theta_{\rm Ni} = 0.48\pi$, $\varphi = 0.35\pi$. Internal fields of magnitude $H_i^{\rm Fe} = 1.05$ kG, $H_i^{\rm Ni} = 10.96$ kG.

films (our Fig. 3), these figures evidence reciprocal frequency behavior as the sign of the wave vector is changed. The effect of inclining the applied magnetic field [i.e., going from Fig. 9(a) to 9(b)] is to eliminate the backward behavior (associated with a negative group velocity) of the dispersion relation of the longitudinal propagation case ($\varphi = 0$) that is present in the in-plane case.

Next we consider a configuration that may be compared with that of Fig. 9 of Ref. [17] that corresponds to a stack of five films, Fe/Ni/Fe/Ni/Fe disposed in a symmetric way, as in Fig. 1. The frequencies of the lowest modes of the structure are plotted as a function of the layer thicknesses (all equal) in Fig. 7. A magnetic field is applied at an oblique angle $\theta = 0.49\pi$ of magnitude $H_0 = 16.94$ kG such that the internal field in Fe is similar to the internal field of Fig. 9 of Ref. [17], that is 1 kG. The parameters of the ferromagnets are: Fe, $4\pi M_s = 21$ kG, $g = 2.1$, $A = 2 \times 10^{-6}$ erg/cm; Ni, $4\pi M_s = 6$ kG, $g = 2.2$, $A = 0.7 \times 10^{-6}$ erg/cm; and an interlayer exchange constant of $A_{12} = 10$ erg/cm^2 is considered. The internal magnetic fields have magnitudes $H_i^{\rm Fe} = 1.05$ kG, $H_i^{\rm Ni} = 10.96$ kG, $\theta_{\rm Fe} = 0.28\pi$, $\theta_{\rm Ni} = 0.48\pi$, $\varphi = 0.35\pi$.Except for the lowest modes, the frequencies come in 2–3 groups that result from lifting of degeneracies due to the interactions in the stack of the two films of Ni and three films of Fe. This is a lifting of degeneracies of exchange-type modes induced by the interlayer exchange interactions included [17]. As far as the dependence of the frequencies on the thickness of the layers shown in Fig. 10, it is a decaying behavior for all modes except for the lowest one of dipolar origin: this is due to their exchange origin, i.e., transverse oscillations across the thickness of the films with a given number of nodes become less energetic as the thickness of the films increases.

Then, we present several figures for a bilayer of equivalent Fe films: frequencies of the lowest modes as a function of the magnitude of the interlayer exchange interaction parameter A_{12}, and plots of the magnetization of selected modes that are shown to evolve as A_{12} changes. The thickness of the Fe layers is 400 Å, $4\pi M_s = 21$ kG, $g = 2.1$. In Fig. 11 we present the frequencies of the lowest dipole-exchange modes of this bilayer of Fe films as a function of the interlayer coupling constant A_{12}. The left figure corresponds to an applied in-plane magnetic field of magnitude $H_0 = 1$ kG, $\varphi = \pi/2$, and the right figure to a magnetic field of magnitude $H_0 = 18.2$ kG applied at an oblique angle $\theta = 0.491\pi$, $\theta_{\rm Fe} = 0.31\pi$, $\varphi = 0.3\pi$, internal field of magnitude $H_i^{\rm Fe} = 0.92$ kG, i.e., an internal magnetic field of similar magnitude as the one of the left figure. Actually the left figure was chosen with the same parameters as those of Fig. 5 of Ref. [17], and it reproduces it. The interpretation of the left figure [17] is that the third mode corresponds to the surface Damon-Eshbach mode of a "full" film of 800 Å, and that the others are exchange modes of 400 Å films at $A_{12} = 0$, and that as A_{12} increases they do split in frequencies between antisymmetriclike modes of higher frequencies and symmetriclike modes that retain their frequencies. Our right figure, which has a quite inclined applied magnetic field (close to $\pi/2$) and with a similar internal field, shows a qualitatively similar behavior than the one of the left figure for an in-plane field, although the

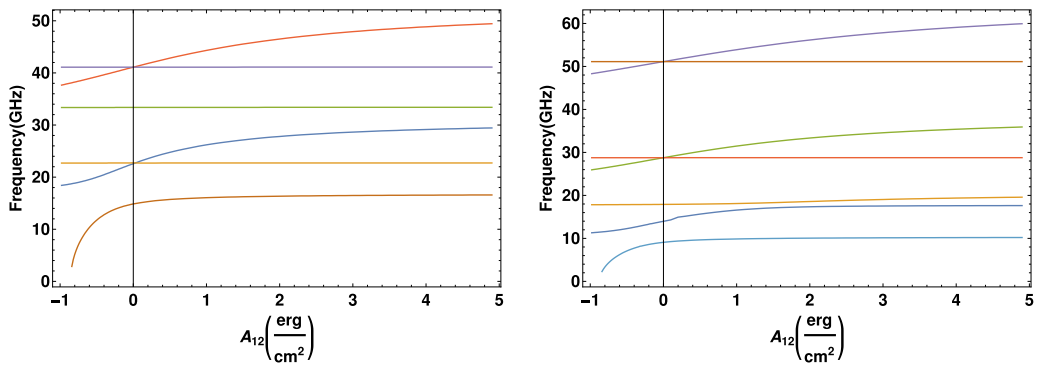

FIG. 11. Frequencies of dipole-exchange modes of a double layer of equivalent Fe films as a function of the interlayer coupling constant A_{12}. Thickness of layers is 400 Å. Left figure: Applied in-plane magnetic field of magnitude $H_0 = 1$ kG, $\varphi = \pi/2$. Right figure: Applied magnetic field of magnitude $H_0 = 18.2$ kG at an oblique angle $\theta = 0.491\pi$, $\theta_{\rm Fe} = 0.31\pi$, $\varphi = 0.3\pi$, internal field of magnitude $H_i^{\rm Fe} = 0.92$ kG.

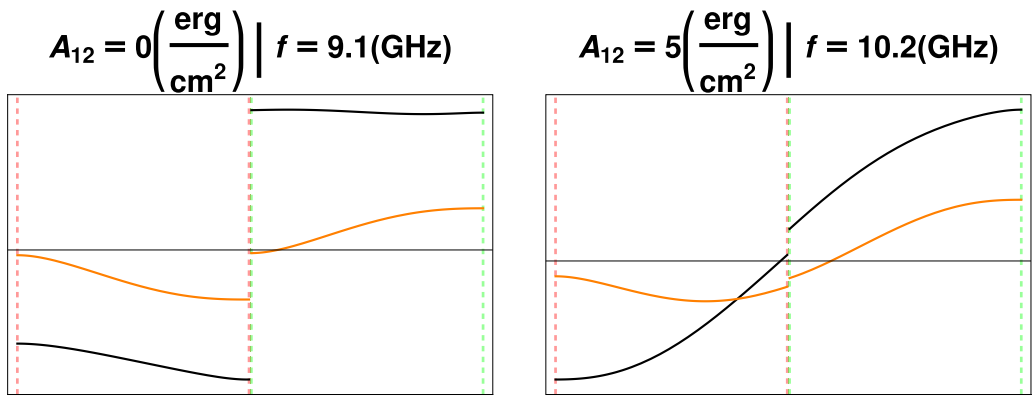

FIG. 12. Magnetization components of the lowest frequency dipole-exchange mode of a double layer of Fe films, for different values of the interlayer coupling constant A_{12}, left figure has $A_{12} = 0$ and right figure $A_{12} = 5$ erg/cm^2 (black curves correspond to m_x, and orange to $m_{\tilde{y}}$). Applied magnetic field of magnitude $H_0 = 18.2$ kG at an oblique angle $\theta = 0.491\pi$, $\theta_{\text{Fe}} = 0.31\pi$, $\varphi = 0.3\pi$. Internal field of magnitude $H_i^{\text{Fe}} = 0.92$ kG, thickness of layers is 400 Å each.

three lowest modes are nondegenerate at $A_{12} = 0$ in this case. In Fig. 12 we present the magnetization components of the lowest frequency dipole-exchange mode of this double layer of equivalent Fe films, for different values of the interlayer coupling constant A_{12}: the left figure corresponds to no interlayer exchange coupling and the right figure to $A_{12} = 5$ erg/cm^2[black curves correspond to m_x, and orange to $m_{\tilde{y}}$, and the parameters correspond to those of Fig. 11(b), i.e., to an obliquely applied magnetic field]. It is seen that with increasing A_{12} the magnetizations of both films become almost coupled continuously into antisymmetriclike modes in this case. In Fig. 13 we present similar plots as in Fig. 12, with the same parameters but now for the magnetization components of the fourth and fifth dipole-exchange modes. The two left figures correspond to the fourth mode, $A_{12} = 0$, $A_{12} = 5$ erg/cm^2, respectively, and the third figure to the fifth mode, $A_{12} = 5$ erg/cm^2 (black curves correspond to m_x, and orange to $m_{\tilde{y}}$). One sees that at increasing A_{12} for the fourth mode the magnetizations of both films become almost coupled continuously into a symmetriclike mode, and that even at $A_{12} = 0$ the continuity was almost there; while the plot for the fifth mode at $A_{12} = 5$ erg/cm^2 shows an antisymmetriclike mode between both films, with not such a good continuity as in the previous case.

Finally, in Fig. 14 we present calculations of dispersion relations of symmetric systems of: (a) three films of Fe-Co-Fe, and (b) five films of Fe-Co-Fe-Co-Fe. These results compare well with Brillouin light scattering (BLS) experimental results presented in Fig. 6 of Ref. [46], but we do the fitting of the experimental results with somewhat different exchange constants: we do use $A_{\text{Fe}} = 2.7 \times 10^{-6}$ erg/cm, $A_{\text{Co}} = 2.1 \times 10^{-6}$ erg/cm, while they did use $A_{\text{Fe}} = 2.1 \times 10^{-6}$ erg/cm, $A_{\text{Co}} = 3.0 \times 10^{-6}$ erg/cm. Notice that there are uncertainties in the literature about the values of these constants, they vary due to the method of measurement, the thickness of the films, environment, etc. For example in Ref. [47], for films of Co of 10 nm they do quote two values for the exchange constant: $A_{\text{Co}} = 1.5 \times 10^{-6}$ erg/cm with a measurement method based on spin spiral formation, and $A_{\text{Co}} = 2.1 \times 10^{-6}$ erg/cm by BLS, which coincides with our estimate. Also, Ref. [48] measured $A_{\text{Co}} = 1.9 \times 10^{-6}$ erg/cm by BLS on Co layers.

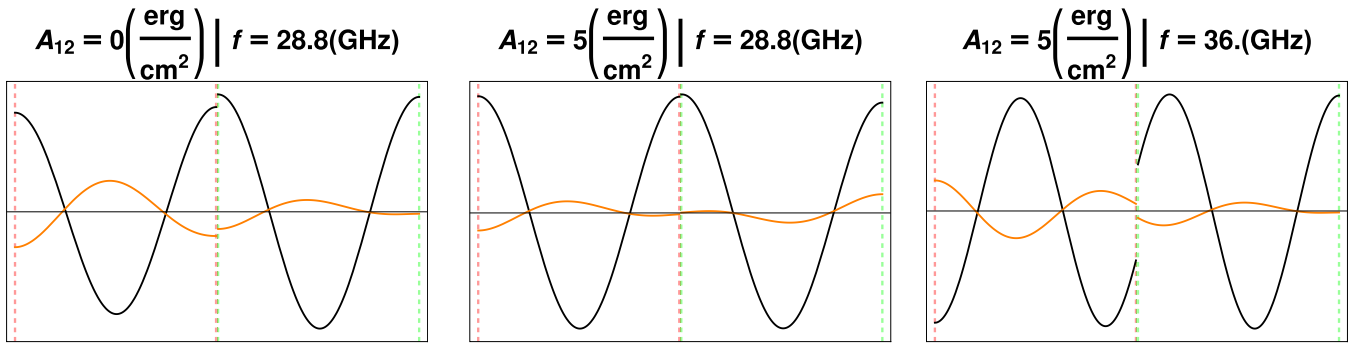

FIG. 13. Magnetization components of the fourth and fifth dipole-exchange mode of a double layer of Fe films, for different values of the interlayer coupling constant A_{12} (black curves correspond to m_x, and orange to m_y). The two left figures correspond to the fourth mode, $A_{12} = 0$, $A_{12} = 5$ erg/cm^2, respectively, and third figure to the fifth mode, $A_{12} = 5$ erg/cm^2. Applied magnetic field of magnitude $H_0 = 18.2$ kG at an oblique angle $\theta = 0.491\pi$, $\theta_{\text{Fe}} = 0.31\pi$, $\varphi = 0.3\pi$. Internal field of magnitude $H_i^{\text{Fe}} = 0.92$ kG, thickness of layers is 400 Å each.

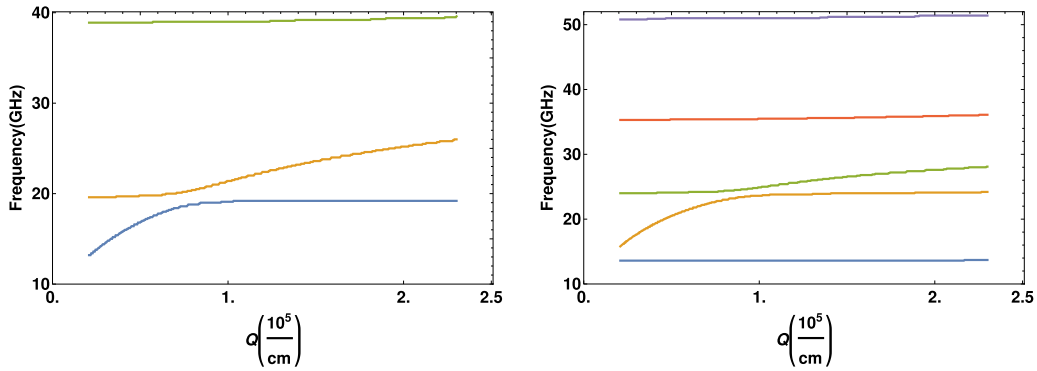

FIG. 14. Dispersion relation of multilayers composed of Fe and Co. (a) Symmetric system of three films of Fe-Co-Fe. (b) Symmetric system of five films Fe-Co-Fe-Co-Fe. The parameters are $M_{\text{Fe}} = 1580$ G, $M_{\text{Co}} = 1450$ G, $g_{\text{Fe}} = 1.99$, $g_{\text{Co}} = 2.1$, $A_{\text{Fe}} = 2.7 \times 10^{-6}$ erg/cm, $A_{\text{Co}} = 2.1 \times 10^{-6}$ erg/cm, $L_{\text{Fe}} = 10$ nm, $L_{\text{Co}} = 20$ nm, magnetic field applied in-plane $H_0 = 500$ Oe, and perpendicular propagation ($\varphi = \pi/2$). In the Fe-Co interfaces there is partial pinning characterized by $K_s \approx 0.4$ erg/cm^2 and the exchange interaction constant between films is $A_{12} \approx 20$ erg/cm^2.

VI. CONCLUSIONS, SUMMARY

We have developed a theory, which is an extension of the Green-extinction theorems, that allows us to calculate with some ease the frequencies and shapes of the magnetostatic and dipole-exchange modes of multilayer structures of ferromagnetic films. If there are N films, one needs to solve a $6N \times 6N$ eigenvalue problem to determine the frequencies of the modes, and the shape of the modes follow by a similar size calculation. This may be done under general conditions with respect to possible boundary conditions at the surfaces of the films (the films may be in contact with nonmagnetic materials or in close proximity with other magnetic materials), and also with respect to the inclination of an applied magnetic field to the structure.

We have presented numerical results for magnetostatic modes and dipole-exchange modes on several structures. Our calculations reproduce old results in the literature, and focus on new results in configurations with inclined applied magnetic fields. In particular, we have shown that for stacks of films which are symmetric with respect to a central plane, modes that propagate in opposite directions have the same frequencies but their shapes are related through specular reflections with respect to the central plane (this is even valid for applied fields in an oblique direction, and with the exchange interaction included). These results are a generalization of the well-known result on Damon-Eshbach magnetostatic surface modes of thin films, i.e., modes that propagate in opposite directions have the same frequency but their shapes attach to the opposite surfaces.

The study of spin wave modes in multilayers has been of interest in part because it provides a way to determine important film parameters, either bulk or surface parameters, or parameters that describe interactions with other films. Thus, we have focused on configurations with an inclination of the applied magnetic field since it brings an experimental degree of freedom that changes frequencies and the shapes of the modes: then it becomes a way of testing the validity of theoretical models, in particular with respect to the appropriate boundary conditions and the strength of surface anisotropies or interaction parameters.

It was already seen in the literature on the topic that there is a very rich variety of spin wave modes in these multilayered ferromagnetic structures: we confirmed and extended this a bit. This rich variety may be exploited to good use in some applications. The multilayers of films are structures of common use, and the method presented in this work is a practical way to determine the details of the spin wave modes in them.

ACKNOWLEDGMENTS

This work was supported by Proyecto Fondecyt 1170781, Chile, and Center for the Development of Nanoscience and Nanotechnology CEDENNA FB0807 (Chile).

APPENDIX: MULTILAYER UNDER AN OBLIQUE APPLIED MAGNETIC FIELD

1. Auxiliary functions

The equations to be solved for the auxiliary functions in the case of an applied magnetic field at an angle θ_H with the planes of the films are the following for film (j):

$$
\begin{aligned}
0 &= \left(-\frac{\partial^2}{\partial y^2} + Q^2\right)\phi_G^{-(\vec{Q},\omega)} - \frac{i}{2}\left(\cos\theta_M^j \frac{\partial}{\partial y} + ik\sin\theta_M^j\right)(M_+^G - M_-^G) - \frac{i}{2}q(M_+^G + M_-^G),\\
0 &= \left[d_j\left(\frac{\partial^2}{\partial y^2} - Q^2\right) - h_{\text{int}}^j + \Omega_j\right]M_+^G + \left(iq + \sin\theta_M^j k - i\cos\theta_M^j \frac{\partial}{\partial y}\right)\phi_G^{-(\vec{Q},\omega)},\\
0 &= \left[d_j\left(\frac{\partial^2}{\partial y^2} - Q^2\right) - h_{\text{int}}^j - \Omega_j\right]M_-^G + \left(iq - \sin\theta_M^j k + i\cos\theta_M^j \frac{\partial}{\partial y}\right)\phi_G^{-(\vec{Q},\omega)}.
\end{aligned}
\tag{A1}
$$

These equations follow from Eqs (5) and (9), and are written in Fourier space, for components $-(\vec{Q},\omega)$, $\vec{Q}=q\hat{x}+k\hat{z}$; $d_j \equiv D_j/4\pi M_s^j$, $h_{\rm int}^j \equiv H_{\rm int}^j/4\pi M_s^j$, $\theta_M \equiv \theta_M^j$, $\Omega_j \equiv \omega/4\pi M_s^j|\gamma_j|$. We look for solutions of exponential form:

$$\phi_I^{-(\vec{Q},\omega)} = Ae^{-\alpha(y-y')}, \quad M_\pm^I = B_\pm e^{-\alpha(y-y')}. \tag{A2}$$

Replacing these previous forms into Eqs. (A1) one obtains the following linear system for A, $B_\pm$:

$$0 = 2(\alpha^2-Q^2)A + i\big(q-\alpha\cos\theta_M^j + ik\sin\theta_M^j\big)B_+ + i\big(q+\alpha\cos\theta_M^j - ik\sin\theta_M^j\big)B_-, \tag{A3}$$

$$0 = \big[d_j(\alpha^2-Q^2) - h_{\rm int}^j + \Omega_j\big]B_+ + i\big(q+\alpha\cos\theta_M^j - ik\sin\theta_M^j\big)A, \tag{A4}$$

$$0 = \big[d_j(\alpha^2-Q^2) - h_{\rm int}^j - \Omega_j\big]B_- + i\big(q-\alpha\cos\theta_M^j + ik\sin\theta_M^j\big)A. \tag{A5}$$

Equations (A4) and (A5) into Eq. (A3) leads to the following equation for α:

$$2(\alpha^2-Q^2) = -\big[\big(k\sin\theta_M^j + i\alpha\cos\theta_M^j\big)^2 + q^2\big]\left(\frac{1}{d_j(\alpha^2-Q^2) - h_{\rm int}^j + \Omega_j} + \frac{1}{d_j(\alpha^2-Q^2) - h_{\rm int}^j - \Omega_j}\right). \tag{A6}$$

For general θ_M^j Eq. (A6) is a sixth order equation for α, then we have in general six different solutions α_n^j for each film (j), with $n=1,\ldots,6$. Notice that if Eq. (A6) for α is written in terms of the variable $iu=\alpha$ it becomes an equation for the roots of a sixth order polynomial in u with real coefficients: by a theorem of algebra it has solutions that come in complex conjugate pairs. Coming back to the variable α this means that there are three solutions with the real part of α positive, and three solutions with their real parts the negatives of the previous values. Once an α_n^j has been determined from Eq. (A6), Eqs. (A4) and (A5) determine the $B_{n\pm}^j$ in terms of the A_n^j:

$$B_{n\pm}^j = -iA_n^j\frac{\big[q\pm\alpha_n^j\cos\theta_M^j \mp ik\sin\theta_M^j\big]}{\big\{d_j\big[\big(\alpha_n^j\big)^2-Q^2\big]-h_{int}^j\pm\Omega_j\big\}} \equiv -iA_n^j b_{n\pm}^j. \tag{A7}$$

The A_n^j become overall multiplicative constant for the auxiliary functions of Eqs. (A2) [Eqs. (A3)–(A5) are homogeneous].

Notice that these solutions, which we call auxiliary functions, are the basis of the so called partial waves method [3,17] used to solve the problem of finding the dipole-exchange modes in single films or multilayers: basically the solution in that case is searched as linear combinations of these partial waves in each submedium, that are matched through the boundary conditions.

2. Magnetostatic modes

The determination of the magnetostatic modes of a multilayer of ferromagnetic films is also possible with this method. If in the case of dipole-exchange modes for every film there were effectively six homogeneous equations and six unknowns to determine the eigenmodes and frequencies at the surfaces (associated with six independent auxiliary functions), in the magnetostatic case there are effectively two equations and two unknowns for each film (two auxiliary functions). The equations for the magnetostatic modes are basically obtained by replacing by zero the exchange constant d_j in the respective equations for the dipole exchange modes. Thus, the extinction Eq. (23) becomes

$$0 = b_y^I(l_2-y')\phi(l_2) - \phi^I(l_2-y')b_y(l_2) - b_y^I(l_1-y')\phi(l_1) + \phi^I(l_1-y')b_y(l_1), \tag{A8}$$

where labels $(\vec{Q},\omega)$ for the modes and $-(\vec{Q},\omega)$ for the auxiliary functions have been omitted. The auxiliary functions have the following exponential form in film (j):

$$\phi_I^{-(\vec{Q},\omega)} = A_j e^{-\alpha_j(y-y')}, \quad M_\pm^I = B_\pm^{(j)}e^{-\alpha_j(y-y')}, \tag{A9}$$

$$b_y^I = [\alpha A_j - i(B_+^{(j)} - B_-^{(j)})\cos\theta_j/2]e^{-\alpha_j(y-y')}, \tag{A10}$$

where from Eq. (A7) one deduces that in the magnetostatic case

$$B_\pm^{(j)} = iA_j\frac{(q\pm\alpha_j\cos\theta_j \mp ik\sin\theta_j)}{h_{int}^j\mp\Omega_j} \equiv -iA_j b_\pm^{(j)}, \tag{A11}$$

and from Eq. (A6) that α_j satisfies a quadratic equation, leading to

$$\alpha_j^{(1,2)} = Q\left(\frac{ih_j\cos\varphi\sin\theta_j\cos\theta_j \pm \sqrt{\big(\Omega_j^2-h_j^2-h_j\big)\big(\Omega_j^2-h_j^2-h_j\sin^2\varphi\cos^2\theta_j\big)}}{h_j^2+h_j\cos^2\theta_j-\Omega_j^2}\right), \tag{A12}$$

[last]i.e., there are two solutions with superindices (1,2), that in $\alpha_j^{(1,2)}$ correspond to signs $+,-$ in Eq. (A12) [it means also that the A_j, $B_\pm^{(j)}$ should have the indices (1,2) since there is one such solution for each $\alpha_j^{(1,2)}$]. Here the wave vector was written as $\vec{Q} = q\hat{x} + k\hat{z} = Q(\sin\varphi\hat{x} + \cos\varphi\hat{z})$. For example, for the in-plane case ($\theta_j = 0$) the previous expression becomes $\alpha_j^2 = q^2 + k^2/\mu_j$, and for the perpendicular to plane case ($\theta_j = \pi/2$), $\alpha_j^2 = \mu_j Q^2$, with $\mu_j = (h_j^2 + h_j - \Omega_j^2)/(h_j^2 - \Omega_j^2)$.

Having clarified how to obtain the auxiliary functions in the magnetostatic case, the remaining task is to combine the extinction equations outside the samples, i.e., Eqs. (16)–(18), with the interior extinction equations for the different films, i.e., Eq. (A8). In the latter process the normal magnetic inductions may be eliminated from these equations, leading to effectively two equations per each film considered, and to an homogeneous eigenvalue problem for the frequencies of the modes and the magnetostatic potentials of these modes evaluated at the surfaces of the films. For example, for two films [(u, d) mean upper and lower films] the magnetostatic extinction equations become [the origin is located symmetrically between the two films, the upper film surfaces are at $y = l$ and at $y = l_u$ (upper one), and the lower film surfaces at $y = -l_d$ (lower one) and $y = -l$]

$$\begin{aligned} 0 = {} & e^{-\alpha_n^u l_u}\left[2\left(\alpha_n^u - Q\right) - \cos\theta_u\left(b_{n+}^u - b_{n-}^u\right)\right]\phi(l_u) \\ & - e^{-\alpha_n^u l}\left\{2\left[\alpha_n^u + Q\coth(2Ql)\right] - \cos\theta_u\left(b_{n+}^u - b_{n-}^u\right)\right\}\phi(l) \\ & + e^{-\alpha_n^u l}\phi(-l)Q/\sinh(2Ql), \end{aligned} \tag{A13}$$

$$\begin{aligned} 0 = {} & e^{\alpha_n^d l}\left\{2\left[\alpha_n^d - Q\coth(2Ql)\right] - \cos\theta_d\left(b_{n+}^d - b_{n-}^d\right)\right\}\phi(-l) \\ & - e^{\alpha_n^d l_d}\left[2\left(\alpha_n^d + Q\right) - \cos\theta_d\left(b_{n+}^d - b_{n-}^d\right)\right]\phi(-l_d) \\ & + e^{\alpha_n^d l}\phi(l)Q/\sinh(2Ql), \end{aligned} \tag{A14}$$

where $n = 1, 2$, and

$$b_{n\pm}^u = -\left(q \pm \alpha_n^u\cos\theta_u \mp ik\sin\theta_u\right)/(h_u \mp \Omega_u), \tag{A15}$$

$$b_{n\pm}^d = -\left(q \pm \alpha_n^d\cos\theta_d \mp ik\sin\theta_d\right)/(h_d \mp \Omega_d). \tag{A16}$$

3. Symmetry considerations

We are interested if there are reciprocal or nonreciprocal relations for the frequencies and modes of multilayers when the wave vector $\vec{k} = q\hat{x} + k\hat{z}$ changes sign, or equivalently $\varphi \to \varphi + \pi$.

a. Analysis of the extinction equations under change of sign of the wave vector

We analyze separately the magnetostatic and dipole-exchange cases.

Magnetostatic modes. If there is a change of sign of the wave vector, let us call the new constant α of the auxiliary functions as $\tilde{\alpha}$. Then, according to Eq. (A12),

$$\tilde{\alpha}^{(1)} = -\alpha^{(2)}, \quad \tilde{\alpha}^{(2)} = -\alpha^{(1)}, \tag{A17}$$

i.e., the new set of $\tilde{\alpha}$ is the negative of the set of α. Now, for a single ferromagnetic film with surfaces at $y = \pm l$ combining Eqs. (17) and (18) with Eq. (A8) leads to the following extinction equations for the magnetostatic modes:

$$\begin{aligned} 0 = {} & e^{-\alpha_n l}[2(\alpha_n - Q) - \cos\theta(b_{n+} - b_{n-})]\phi(l) \\ & - e^{\alpha_n l}[2(\alpha_n + Q) - \cos\theta(b_{n+} - b_{n-})]\phi(-l), \end{aligned} \tag{A18}$$

where $n = 1, 2$, and

$$b_{n\pm} = -(q \pm \alpha_n\cos\theta \mp ik\sin\theta)/(h \mp \Omega). \tag{A19}$$

In changing the sign of the wave vector, the sets of α and $b_\pm$ change signs, and Eq. (A18) becomes

$$\begin{aligned} 0 = {} & -e^{\alpha_n l}[2(\alpha_n + Q) - \cos\theta(b_{n+} - b_{n-})]\phi(l) \\ & + e^{-\alpha_n l}[2(\alpha_n - Q) - \cos\theta(b_{n+} - b_{n-})]\phi(-l), \end{aligned} \tag{A20}$$

i.e., the frequencies are reciprocal $\omega(\vec{k}) = \omega(-\vec{k})$ [the determinants resulting from Eqs. (A18) and (A20) are equivalent], but the modes are specularly related [$\phi(\pm l) \to \phi(\mp l)$].

Similarly, one may analyze the case of magnetostatic modes in two films changing $\vec{k} \to -\vec{k}$ in Eqs. (A12)–(A16): one sees that if the films are different (either in geometry or materials) there are no symmetry relations (this is seen for example in Fig. 5), but if the films are of the same dimensions and the same type there is still reciprocity in frequencies and the modes are specularly related, as it is seen in Fig. 3. One may generalize these results to stacks of films, if the stack is specularly symmetric with respect to a given plane the frequencies are reciprocal and the modes are specularly related, this is seen for example in Fig. 7.

In the following subsection on dipole-exchange modes we discuss the underlying symmetry that explains the previous results, since the analysis for magnetostatic modes is analogous.

Dipole-exchange modes. In the case of dipole-exchange modes if the sign of the wave vector is changed in Eq. (A6) for the paramater α, and at the same type α is changed into $-\alpha$, the equation remains unchanged, meaning that the new set of solutions $\tilde{\alpha}$ are the negatives of the α, as occurred in the magnetostatic case. Now we consider a single ferromagnetic film, and to be specific we consider boundary conditions associated with partial pinning, i.e.,

$$\frac{\partial M_\pm}{\partial n} = -\lambda\sin^2\theta M_\pm \pm \frac{\lambda}{2}\cos^2\theta(M_+ - M_-). \tag{A21}$$

The extinction Eq. (26) in this case become

$$\begin{aligned} 0 = {} & e^{-\alpha_n l}[2(\alpha_n - Q) - \cos\theta(b_{n+} - b_{n-})]\phi(l)f - e^{\alpha_n l}[2(\alpha_n + Q) - \cos\theta(b_{n+} - b_{n-})]\phi(-l) \\ & + e^{-\alpha_n l}\{[(\lambda\sin^2\theta - \alpha_n)b_{n-} + (\lambda/2)\cos^2\theta(b_{n+} - b_{n-})]\tilde{M}_+(l) + [(\lambda\sin^2\theta - \alpha_n)b_{n+} - (\lambda/2)\cos^2\theta(b_{n+} - b_{n-})]\tilde{M}_-(l)\} \\ & + e^{\alpha_n l}\{[(\lambda\sin^2\theta + \alpha_n)b_{n-} + (\lambda/2)\cos^2\theta(b_{n+} - b_{n-})]\tilde{M}_+(-l) + [(\lambda\sin^2\theta + \alpha_n)b_{n+} - (\lambda/2)\cos^2\theta(b_{n+} - b_{n-})]\tilde{M}_-(-l)\}, \end{aligned} \tag{A22}$$

where $\tilde{M}_\pm \equiv -idM_\pm$, and $n = 1, \ldots, 6$, and

$$b_{n\pm} = (q \pm \alpha_n \cos\theta \mp ik \sin\theta)/(d(\alpha_n^2 - Q^2) - h \pm \Omega). \tag{A23}$$

If one changes the sign of $\vec{Q}$, i.e., of q and k, the sets of α and the $b_\pm$ change sign, and as for the magnetostatic case, the new equations are equivalent to the set of Eq. (A22) leading to reciprocal frequencies, but the variables have been "specularly reflected" with respect to the plane $y = 0$ in the following way: $\phi(\pm l), M_+(\pm l), M_-(\pm l) \to \phi(\mp l), -M_($ $\mp l), -M_-(\mp l)$.

Now, following a similar analysis as in the magnetostatic case one may conclude in the dipole-exchange case that for a pair of inequivalent films the frequency dispersion relations as well as the modes are nonreciprocal, but if the two films are equivalent the frequencies are reciprocal (as in Fig. 9) and the potential and magnetizations of the modes are specularly reflected symmetrically for the potential and antisymmetrically for the magnetizations, as in the single film case just explained. And again, as in the magnetostatic case, one concludes that a stack of films that is symmetric in all its properties with respect to a specular reflection with respect to a given central plane, then the frequencies are reciprocal and the modes are specularly reflected in a symmetric way for the potentials and antisymmetrically for the magnetizations.

b. Underlying symmetry, derivation of modes reciprocal in frequencies and nonreciprocal in shapes

The underlying symmetry that explains the previous results is associated with the fact that for a symmetric stack of films (with respect to a central plane) if one applies the dc magnetic field in the opposite direction and analyzes the modes with respect to inverted axes one should get the same frequencies and same modes in the new reference frame since under this change the system is equivalent to the original one. We elaborate about this in the following. The linear version of the Landau-Lifshitz equation in a given film (j), i.e., Eq. (9), read $(\partial/\partial\tilde{y} = \cos\theta\partial/\partial y - \sin\theta\partial/\partial z)$:

$$i\Omega m_{\tilde{y}} = d\nabla^2_{\vec{x}} m_x - \frac{1}{4\pi}\frac{\partial\phi}{\partial x} - h_i m_x, \tag{A24}$$

$$i\Omega m_x = -d\nabla^2_{\vec{x}} m_{\tilde{y}} + \frac{1}{4\pi}\left(\cos\theta\frac{\partial\phi}{\partial y} - \sin\theta\frac{\partial\phi}{\partial z}\right) + h_i m_{\tilde{y}}, \tag{A25}$$

with h_i the normalized magnitude of the internal field, and we do not write indices (j) associated with the given film. The equations for the magnetostatic potential in magnetic and nonmagnetic regions are, respectively:

$$0 = \nabla^2_{\vec{x}}\phi - 4\pi(\partial m_x/\partial x + \partial m_{\tilde{y}}/\partial\tilde{y}), \tag{A26}$$

$$0 = \nabla^2_{\vec{x}}\phi. \tag{A27}$$

These equations are to be solved subject to boundary conditions of magnetostatic and exchange origin. We will assume that there is a mode $\tilde{m}_x, \tilde{m}_{\tilde{y}}, \tilde{\phi}$, with frequency $\tilde{\omega}$ that satisfies these equations and boundary conditions. Now, if the original axis are (x, y, z), we call the inverted axis $(X, Y, Z) = (-x, -y, -z)$. Then the equivalent of Eq. (9) in a given film with an inverted dc field and in the inverted frame read

$$i\Omega M_{\tilde{Y}} = d\nabla^2_{\vec{X}} M_X - \frac{1}{4\pi}\frac{\partial\Phi}{\partial X} - h_i M_X, \tag{A28}$$

$$i\Omega M_X = -d\nabla^2_{\vec{X}} M_{\tilde{Y}} + \frac{1}{4\pi}\left(\cos\theta\frac{\partial\Phi}{\partial Y} - \sin\theta\frac{\partial\Phi}{\partial Z}\right) + h_i M_{\tilde{Y}}, \tag{A29}$$

and the associated magnetostatic equations are

$$0 = \nabla^2_{\vec{X}}\Phi - 4\pi(\partial M_X/\partial X + \partial M_{\tilde{Y}}/\partial\tilde{Y}), \tag{A30}$$

$$0 = \nabla^2_{\vec{X}}\Phi. \tag{A31}$$

Now these previous equations and boundary conditions are solved by modes of the same form and frequencies as the ones for the original problem, i.e.,

$$i\tilde{\Omega}\tilde{m}_{\tilde{y}}(\vec{X}) = d\nabla^2_{\vec{X}}\tilde{m}_x - \frac{1}{4\pi}\frac{\partial\tilde{\phi}}{\partial X} - h_i\tilde{m}_x, \tag{A32}$$

$$i\tilde{\Omega}\tilde{m}_x(\vec{X}) = -d\nabla^2_{\vec{X}}\tilde{m}_{\tilde{y}} + \frac{1}{4\pi}\left(\cos\theta\frac{\partial\tilde{\phi}}{\partial Y} - \sin\theta\frac{\partial\tilde{\phi}}{\partial Z}\right) + h_i\tilde{m}_{\tilde{y}}, \tag{A33}$$

$$0 = \nabla^2_{\vec{X}}\tilde{\phi} - 4\pi(\partial\tilde{m}_x/\partial X + \partial\tilde{m}_{\tilde{y}}/\partial\tilde{Y}), \tag{A34}$$

$$0 = \nabla^2_{\vec{X}}\tilde{\phi}, \tag{A35}$$

with all the fields evaluated at $\vec{X} = (X, Y, Z)$. Changing variables according to $(X, Y, Z) = (-x, -y, -z)$, one gets

$$i\tilde{\Omega}\tilde{m}_{\tilde{y}}(-\vec{x}) = d\nabla^2_{\vec{x}}\tilde{m}_x + \frac{1}{4\pi}\frac{\partial\tilde{\phi}}{\partial x} - h_i\tilde{m}_x, \tag{A36}$$

$$i\tilde{\Omega}\tilde{m}_x(-\vec{x}) = -d\nabla^2_{\vec{x}}\tilde{m}_{\tilde{y}} - \frac{1}{4\pi}\left(\cos\theta\frac{\partial\tilde{\phi}}{\partial y} - \sin\theta\frac{\partial\tilde{\phi}}{\partial z}\right) + h_i\tilde{m}_{\tilde{y}}, \tag{A37}$$

$$0 = \nabla^2_{\vec{x}}\tilde{\phi} + 4\pi(\partial\tilde{m}_x/\partial x + \partial\tilde{m}_{\tilde{y}}/\partial\tilde{y}), \tag{A38}$$

$$0 = \nabla^2_{\vec{x}}\tilde{\phi}, \tag{A39}$$

with all the fields now evaluated at $-\vec{x} = (-x, -y, -z)$. Thus, if the mode $\tilde{\phi}(\vec{x})$, $\tilde{m}_x(\vec{x})$, $\tilde{m}_{\tilde{y}}(\vec{x})$ is a solution of the original Eqs. (A24)–(A27) at frequency $\tilde{\omega}$, then comparing Eqs. (A36)–(A39) with Eqs. (A24)–(A27) one concludes that $\tilde{\phi}(-\vec{x})$, $-\tilde{m}_x(-\vec{x})$, $-\tilde{m}_{\tilde{y}}(-\vec{x})$ is a solution of the original Eqs. (A24)–(A27) at frequency $\tilde{\omega}$, or a mode of those equations that correspond to an applied magnetic field in the original direction (for brevity we left out the discussion of the boundary conditions, but the conclusion is not affected by them). Thus, we have proved that for a symmetric stack of films, with a magnetic field applied in an arbitrary direction, there are modes with reciprocal frequencies and nonreciprocal in shape: their magnetic potentials are symmetric and magnetization components antisymmetric with respect to specular reflections with respect to the central plane of symmetry of the stack of films.

4. Contributions to boundary conditions

a. Intralayer exchange

With respect to a contribution from the internal exchange interaction within a material to the boundary condition at one of its surfaces, the internal exchange interaction may be written as

$$E_X = \frac{A}{M_s^2}\int dV \sum_j (\nabla M_j)^2. \tag{A40}$$

Taking the variation of the previous expression:

$$\begin{aligned}\delta E_X &= 2\frac{A}{M_s^2}\sum_j \int dV \nabla M_j \cdot \nabla(\delta M_j)\\ &= 2\frac{A}{M_s^2}\sum_j \int dV [\nabla\cdot(\delta M_j \nabla M_j) - \nabla\cdot(\nabla M_j)\delta M_j]\\ &= -2\frac{A}{M_s^2}\sum_j \int dV \nabla^2 M_j \delta M_j + 2\frac{A}{M_s^2}\sum_j \int d\vec{S}\cdot\nabla M_j\\ &= \delta M_j,\end{aligned} \tag{A41}$$

which allows us to identify the following volumetric exchange effective field:

$$\vec{H}_X^{\text{vol}} = -\delta E_X/\delta\vec{M} = \frac{2A}{M_s^2}\nabla^2\vec{M} = \frac{D}{M_s}\nabla^2\vec{M}, \tag{A42}$$

and also the following superficial effective exchange field:

$$\vec{H}_X^{\text{sup}} = -\frac{2A}{M_s^2}\frac{\partial\vec{M}}{\partial n}. \tag{A43}$$

Notice that here n represents a normal that points to the outside of the material. The previous result may also be obtained by integrating the volumetric exchange field of Eq. (A42) over a small volume ΔV on the edge of the sample (that has a part outside the sample, this is the volume used by Rado-Weertman to deduce their boundary conditions). Since $\nabla^2\phi = \nabla\cdot\nabla\phi$ one may use the divergence theorem to deduce that

$$\int_{\Delta V} dV \frac{2A}{M_s^2}\nabla^2 M_j = -\frac{2A}{M_s^2}\int_S \nabla M_j\cdot d\vec{S} = -\frac{2A}{M_s^2}\int_S \frac{\partial M_j}{\partial n} dS, \tag{A44}$$

with the minus sign coming from the fact that the external normal to ΔV has the opposite direction of the external normal to the material, i.e., it is consistent with the result of Eq. (A43), and explains the first term of Eq. (33) that was derived by Rado-Weertman [19].

b. Surface anisotropy

The surface anisotropy energy has the form $E_{\text{an}}^s = \int dS K_s[1-(\vec{M}\cdot\hat{n}/M_s)^2]$, its variation leads to and effective field acting at the surface that is

$$-\frac{\delta E_{\text{an}}^s}{\delta\vec{M}} = \frac{2K_s}{M_s^2}(\vec{M}\cdot\hat{n})\hat{n}. \tag{A45}$$

When this is replaced appropriately in Eq. (33) for the balance of superficial torques on the surface of one film, one obtains

$$0 = \vec{M}\times\left\{-\frac{\partial\vec{M}}{\partial n} + \lambda(\vec{M}\cdot\hat{n})\hat{n}\right\}, \tag{A46}$$

with $\lambda = K_s/A$. By replacing a linear approximation for the magnetization in Eq. (A46), i.e., $\vec{M}\simeq M_s\hat{\tilde{z}} + m_{\tilde{y}}\hat{\tilde{y}} + m_x\hat{x}$, one obtains for the linear terms:

$$0 = \frac{\partial m_{\tilde{y}}}{\partial n}\hat{x} - \frac{\partial m_x}{\partial n}\hat{\tilde{y}} + \lambda[-\cos(2\theta)m_{\tilde{y}}\hat{x} + m_x\sin\theta\hat{z}]. \tag{A47}$$

Finally, doing an approximation that neglects a term in the $\hat{\tilde{z}}$ direction coming from the last term of the previous equation, one gets the boundary conditions of Eqs. (34) and (35), that were derived in Ref. [20].

c. Interlayer exchange

We derive the boundary conditions Eqs. (45) and (46) associated with the interlayer exchange interaction of Eq. (43). According to the Rado-Weertman criteria of Eq. (33), we impose the total surface effective torques at the surfaces $y = \pm a/2$ (simplified as just $\pm$, a is a lattice constant) to be null, and this leads to

$$0 = -\frac{2A_1}{M_1^2}\vec{M}_1^-\times\frac{\partial\vec{M}_1^-}{\partial y} + A_{12}\vec{M}_1^-\times\vec{M}_2^+, \tag{A48}$$

$$0 = \frac{2A_2}{M_2^2}\vec{M}_2^+\times\frac{\partial\vec{M}_2^+}{\partial y} + A_{12}\vec{M}_2^+\times\vec{M}_1^-. \tag{A49}$$

Also we may approximate

$$\vec{M}_1^- \simeq \vec{M}_1^{0-} - \frac{a}{2}\frac{\partial\vec{M}_1^{0-}}{\partial y}, \tag{A50}$$

$$\vec{M}_2^+ \simeq \vec{M}_2^{0+} + \frac{a}{2}\frac{\partial\vec{M}_2^{0+}}{\partial y}. \tag{A51}$$

Subtracting Eq. (A48) from Eq. (A49) leads to Eq. (45) [where one has also used Eqs. (A50) and (A51)]. Also, adding Eqs. (A48) and (A49) leads to Eq. (46).

Now we write the linear versions of Eqs. (A48) and (A49), using that

$$\vec{M}_{1,2}\simeq M_{1,2}\hat{u}_{1,2} + m_x^{(1,2)}\hat{x} + m_\eta^{(1,2)}\hat{\eta}_{1,2}, \tag{A52}$$

where we have used the notation $\hat{u}_{1,2} = \hat{\tilde{z}}_{1,2}$ for the direction of the equilibrium magnetization in each medium, and $\hat{\eta}_{1,2} = \hat{\tilde{y}}_{1,2}$ as the perpendicular direction to it (and to $\hat{x}$). Equations (A50) and (A51) in Eq. (A48) lead when projected into the $\hat{\eta}_1$ and $\hat{x}$ directions to

$$\begin{aligned}0 = &-\frac{2A_1}{M_1}\frac{\partial m_x^{(1)}}{\partial y} + A_{12}\left(M_1 m_x^{(2)} - M_2\cos\Delta\theta m_x^{(1)}\right)\\ &+\frac{aA_{12}}{2}\left(M_2\cos\Delta\theta\frac{\partial m_x^{(1)}}{\partial y} + M_1\frac{\partial m_x^{(2)}}{\partial y}\right),\end{aligned} \tag{A53}$$

$$\begin{aligned}0 = &\frac{2A_1}{M_1}\frac{\partial m_\eta^{(1)}}{\partial y} + A_{12}\cos\Delta\theta\left(M_2 m_\eta^{(1)} - M_1 m_\eta^{(2)}\right)\\ &-\frac{aA_{12}}{2}\cos\Delta\theta\left(M_2\frac{\partial m_\eta^{(1)}}{\partial y} + M_1\frac{\partial m_\eta^{(2)}}{\partial y}\right),\end{aligned} \tag{A54}$$

with $\Delta\theta = \theta_2 - \theta_1$. Equation (A53) contains an approximation, the terms proportional to $\cos\Delta\theta$ result from a projection of terms proportional to $\hat{\eta}_2$ into $\hat{\eta}_1$. Now, Eqs. (A50) and (A51) in Eq. (A49) lead when projected into the $\hat{\eta}_2$ and $\hat{x}$

directions to

$$0 = \frac{2A_2}{M_2}\frac{\partial m_x^{(2)}}{\partial y} + A_{12}\left(M_2 m_x^{(1)} - M_1 \cos\Delta\theta m_x^{(2)}\right) - \frac{aA_{12}}{2}\left(M_1 \cos\Delta\theta \frac{\partial m_x^{(2)}}{\partial y} + M_2 \frac{\partial m_x^{(1)}}{\partial y}\right), \quad \text{(A55)}$$

$$0 = -\frac{2A_2}{M_2}\frac{\partial m_\eta^{(2)}}{\partial y} + A_{12}\cos\Delta\theta\left(M_1 m_\eta^{(2)} - M_2 m_\eta^{(1)}\right) + \frac{aA_{12}}{2}\cos\Delta\theta\left(M_1 \frac{\partial m_\eta^{(2)}}{\partial y} + M_2 \frac{\partial m_\eta^{(1)}}{\partial y}\right). \quad \text{(A56)}$$

Equation (A55) contains an approximation, the terms proportional to $\cos\Delta\theta$ result from a projection of terms proportional to $\hat{\eta}_1$ into $\hat{\eta}_2$.

Equations (A53)–(A56) may be regarded as four equations for the four unknowns $\partial m_x^{(1,2)}/\partial y$, $\partial m_\eta^{(1,2)}/\partial y$: through a matrix inversion one may then express each of these unknowns in terms of the magnetization components $m_x^{(1,2)}$ and $m_\eta^{(1,2)}$. This information is then replaced in the extinction equations and one proceeds with the method in order to calculate the eigenfrequencies and eigenmodes.

[1] R. W. Damon and J. R. Eshbach, J. Phys. Chem. Solids **19**, 308 (1961).
[2] M. J. Hurben and C. E. Patton, J. Magn. Magn. Mater. **139**, 263 (1995).
[3] R. E. De Wames and T. Wolfram, J. Appl. Phys. **41**, 987 (1970).
[4] B. A. Kalinikos and A. N. Slavin, J. Phys. C: Solid State Phys. **19**, 7013 (1986).
[5] A. Kreisel, F. Sauli, L. Bartosch, and P. Kopietz, Eur. Phys. J. B **71**, 59 (2009).
[6] G. Li, C. Sun, T. Nattermann, and V. L. Pokrovsky, Phys. Rev. B **98**, 014436 (2018).
[7] C. Sun, T. Natternmann, and V. L. Pokrovsky, J. Phys. D: Appl. Phys. **50**, 143002 (2017).
[8] P. Grunberg and K. Mika, Phys. Rev. B **27**, 2955 (1983).
[9] R. E. Camley, T. S. Rahman, and D. L. Mills, Phys. Rev. B **27**, 261 (1983).
[10] B. Hillebrands, P. Baumgart, R. Mock, G. Guntherodt, A. Boufelfel, and C. M. Falco, Phys. Rev. B **34**, 9000 (1986).
[11] K. Vayhinger and H. Kronmuller, J. Magn. Magn. Mater. **62**, 159 (1986).
[12] B. Heinrich, S. T. Purcell, J. R. Dutcher, K. B. Urquhart, J. F. Cochran, and A. S. Arrott, Phys. Rev. B **38**, 12879 (1988).
[13] K. Vayhinger and H. Kronmuller, J. Magn. Magn. Mater. **72**, 307 (1988).
[14] B. Hillebrands, Phys. Rev. B **37**, 9885 (1988).
[15] M. Vohl, J. Barnas, and P. Grunberg, Phys. Rev. B **39**, 12003 (1989).
[16] J. Barnas and P. Grunberg, J. Magn. Magn. Mater. **82**, 186 (1989).
[17] B. Hillebrands, Phys. Rev. B **41**, 530 (1990).
[18] R. L. Stamps and B. Hillebrands, Phys. Rev. B **44**, 5095 (1991).
[19] G. T. Rado and J. R. Weertman, J. Phys. Chem. Solids **11**, 315 (1959).
[20] R. F. Soohoo, Phys. Rev. **131**, 594 (1963).
[21] F. Hoffmann, Phys. Status Solidi B **41**, 807 (1970).
[22] F. Hoffmann, A. Stankoff, and H. Paskard, J. Appl. Phys. **41**, 1022 (1970).
[23] K. M. Pashaev and D. L. Mills, Phys. Rev. B **43**, 1187 (1991).
[24] J. F. Cochran and B. Heinrich, Phys. Rev. B **45**, 13096 (1992).
[25] J. Barnas, J. Magn. Magn. Mater. **102**, 319 (1991).
[26] D. L. Mills, Phys. Rev. B **45**, 13100 (1992).
[27] A. N. Slavin, I. V. Rojdestvenski, and M. G. Cottam, J. Appl. Phys. **76**, 6549 (1994).
[28] S. Demokritov and E. Tsymbal, J. Phys.: Condens. Matter **6**, 7145 (1994).
[29] R. Zivieri, P. Vavassori, L. Giovannini, F. Nizzoli, E. E. Fullerton, M. Grimsditch, and V. Metlushko, Phys. Rev. B **65**, 165406 (2002).
[30] R. L. Stamps, Phys. Rev. B **49**, 339 (1994).
[31] M. Buchmeier, B. K. Kuanr, R. R. Gareev, D. E. Burgler, and P. Grunberg, Phys. Rev. B **67**, 184404 (2003).
[32] M. Buchmeier, H. Dassow, D. E. Burgler, and C. M. Schneider, Phys. Rev. B **75**, 184436 (2007).
[33] S. A. Nikitov, Ph. Tailhades, C. S. Tsai, J. Magn. Magn. Mater. **236**, 320 (2001).
[34] R. E. Camley and R. L. Stamps, J. Phys.: Condens. Matter **5**, 3727 (1993).
[35] J. Barnas, in *Linear and Nonlinear Spin Waves in Magnetic Films and Superlattices*, edited by M. G. Cottam (World Scientific, Singapore, 1994), Chap. 3.
[36] Z. Zhi-Dong, in *Handbook of Thin Film Materials*, Vol. 5: Nanomaterials and Magnetic Thin Films, edited by H. S. Nalwa (Academic, New York, 2002), Chap. 4.
[37] R. E. Arias, Phys. Rev. B **94**, 134408 (2016).
[38] F. Toigo, A. Marvin, V. Celli, and N. R. Hill, Phys. Rev. B **15**, 5618 (1977).
[39] D. L. Mills and E. Burstein, Rep. Prog. Phys. **37**, 817 (1973).
[40] R. Arias and D. L. Mills, Phys. Rev. B **70**, 094414 (2004).
[41] R. E. Camley, Surf. Sci. Rep. **7**, 103 (1987).
[42] A. G. Gurevich and G. A. Melkov, *Magnetization Oscillations and Waves* (CRC, Boca Raton, FL, 1996).
[43] R. Magaraggia, K. Kennewell, M. Kostylev, R. L. Stamps, M. Ali, D. Greig, B. J. Hickey, and C. H. Marrows, Phys. Rev. B **83**, 054405 (2011).
[44] M. Kostylev, J. Appl. Phys. **115**, 233902 (2014).
[45] V. V. Kruglyak, O. Y. Gorobets, Y. I. Gorobets, and A. N. Kuchko, J. Phys.: Condens. Matter **26**, 406001 (2014).
[46] L. Giovannini, S. Tacchi, G. Gubbiotti, G. Carlotti, F. Casoli, and F. Albertini, J. Phys.: Condens. Matter **17**, 6483 (2005).
[47] C. Eyrich, W. Huttema, M. Arora, E. Montoya, F. Rashidi, C. Burrowes, B. Kardasz, E. Girt, B. Heinrich, O. N. Mryasov, M. From, and O. Karis, J. Appl. Phys. **111**, 07C919 (2012).
[48] S. P. Vernon, S. M. Lindsay, and M. B. Stearns, Phys. Rev. B **29**, 4439 (1984).